CAPITAL UNIVERSITY OF SCIENCE AND TECHNOLOGY, ISLAMABAD

Seamless Synchronization of Synchronverter with an Unbalanced Grid

by

Faisal Waseem

A thesis submitted in partial fulfillment for the degree of Master of Science

in the

Faculty of Engineering
Department of Electrical and Computer Engineering

2024

Dedicated to my better half, Sadia Hanif

CERTIFICATE OF APPROVAL

Seamless Synchronization of Synchronverter with an Unbalanced Grid

by

Faisal Waseem

(MEE221006)

THESIS EXAMINING COMMITTEE

S. No.	Examiner	Name	Organization
(a)	External Examiner	Dr. Kamran Hafeez	COMSATS, Islamabad
(b)	Internal Examiner	Dr. Muhammad Ashraf	CUST, Islamabad
(c)	Supervisor	Dr. Muhammad Naeem	CUST, Islamabad

Dr. Muhammad Naeem
Thesis Supervisor
August, 2024

Dr. Noor Muhammad Khan
Head
Dept. of Electrical and Computer Engineering
August, 2024

Dr. Imtiaz Ahmad Taj
Dean
Faculty of Engineering
August, 2024

Author's Declaration

I, **Faisal Waseem** hereby state that my MS thesis titled "**Seamless Synchronization of Synchronverter with an Unbalanced Grid**" is my own work and has not been submitted previously by me for taking any degree from Capital University of Science and Technology, Islamabad or anywhere else in the country/abroad.

At any time if my statement is found to be incorrect even after my graduation, the University has the right to withdraw my MS Degree.

(Faisal Waseem)

Registration No: MEE221006

Plagiarism Undertaking

I solemnly declare that research work presented in this thesis titled "**Seamless Synchronization of Synchronverter with an Unbalanced Grid**" is solely my research work with no significant contribution from any other person. Small contribution/help wherever taken has been duly acknowledged and that complete thesis has been written by me.

I understand the zero tolerance policy of the HEC and Capital University of Science and Technology towards plagiarism. Therefore, I as an author of the above titled thesis declare that no portion of my thesis has been plagiarized and any material used as reference is properly referred/cited.

I undertake that if I am found guilty of any formal plagiarism in the above titled thesis even after award of MS Degree, the University reserves the right to withdraw/revoke my MS degree and that HEC and the University have the right to publish my name on the HEC/University website on which names of students are placed who submitted plagiarized work.

(Faisal Waseem)

Registration No: MEE221006

Acknowledgement

All praises to Allah Who created me and taught me what I didn't know. I am grateful to my supervisor Dr. Muhammad Naeem who rectified the framework of this thesis and guided me throughout my research. I also thank him for the support and motivation he provided during the hard times of this research. He helped in the writeup of publications and continuously backed me up to improve and resubmit the publications.

I am thankful to the Head of my department, Dr. Noor Muhammad Khan, who allowed me to complete my research with dedication. He supported me in managing departmental tasks and responsibilities throughout the degree duration. Thanks to my friends and colleagues at CUST for being well wishers. Finally, special thanks to my family who allowed me to complete this research without creating disturbances.

Faisal Waseem

Abstract

The increasing demand for energy, depletion of conventional fuel reserves, and growing environmental concerns have shifted the focus within the power grid from conventional resources to renewable energy sources. This trend has driven the evolution of the power system towards the smart grid, employing power electronic converters that lack inertia, thereby posing challenges to the voltage and frequency stability of the power system. To address this issue, researchers are promoting the concept of Virtual Synchronous Machines (VSM). VSM allows power electronic converters to replicate the characteristics of traditional synchronous generators, thereby supporting the future power grid. Among VSMs, the synchronverter, an inverter that emulates a real synchronous generator, stands out due to its simplicity and inertial dynamics. Like conventional synchronous generators, it has the ability to maintain frequency and voltage in the power grid.

The synchronverter is capable of staying synchronized with the grid without the need for a dedicated synchronization unit. It can seamlessly do transition from grid-connected to standalone mode without requiring any adjustments to the controller. However, it does require a synchronizer to monitor the grid's phase and frequency as a reference before connecting to the grid. Researchers have put forward several schemes for the initial synchronization of the synchronverter to the grid. Due to the complexity, inefficiency, and decreasing performance of the phase-locked loop (PLL) in a weak grid, alternative PLL-less synchronization methods are proving to be a superior choice. Many PLL-less schemes with hot-seamless synchronization feature are designed for ideally balanced grid, which is not available in all distribution networks. The unbalance in power grid is more common in weak grid areas where single phase loads can easily cause an unbalance.

In this research a method of positive sequence extraction is implemented in a PSE block and then embedded in an existing PLL-less Fourier Analysis based self-synchronizer. The PSE block extracts the instantaneous positive sequence voltages of an unbalanced grid by employing the Fortescue and Lyon transformation method. The proposed synchronizer during pre-synchronizing (a) ensures

hot-seamless transfer of synchronverter from standalone to grid-connected mode (b) significantly reduces the voltage difference and inrush currents while power grid has an unbalance in voltage (c) prevents over current tripping of synchronverter by reducing large inrush currents while power grid has an unbalance in phase angle (d) provides capability of riding through an unbalanced sag during pre-synchronization process. The proposed scheme is designed, validated by simulations in MATLAB/Simulink and compared with the existing PLL-Less Fourier Analysis Based Self-synchronizer.

Contents

List of Figures

List of Tables

Abbreviations

AEDB	Alternative Energy Development Board
DG	Distributed Generation
DFIG	Doubly-Fed Induction Generator
DRMSV	Differential Root Mean Square Voltage
EV	Electric Vehicle
ESD	Energy Storage Device
ESS	Energy Storage System
EPLL	Enhanced Phase-Locked Loop
PSE	Positive Sequence Extractor
HVDC	High Voltage Direct Current
IPP	Independent Power Producer
LVDC	Low Voltage Direct Current
MPP	Maximum Power Point
MPPT	Maximum Power Point Tracking
NIST	National Institute of Silicon Technology
NTDC	National Transmission and Dispatch Company
NEPRA	National Electric Power Regulatory Authority
PV	Photo-Voltaic
PHEV	Plug-in Hybrid Electric Vehicle
PEC	Power Electronic Converter
PLL	Phase-Locked Loop
PWM	Pulse Width Modulation
POV	Point-of-View

PI	Proportional Integral
RER	Renewable Energy Resource
ROCOF	Rate-of-Change-of-Frequency
RMS	Root Mean Square
SG	Conventional Synchronous Generator
SM	Synchronous Machine
SPP	Solar Power Plant
SPC	Synchronous Power Controller
SOC	State-of-Charge
STATCOM	Static Compensator
SVC	Static Var Compensator
VSM	Virtual Synchronous Machine
VSG	Virtual Synchronous Generator
VSC	Voltage Source Converter
VCO	Voltage Controlled Oscillator
V2G	Vehicle-to-Grid

Symbols

Symbol	Name	Unit
Φ_s	Stator flux linkage	
Φ_f	Rotor flux linkage	
i_a, i_b, i_c	Stator windings currents	
i_f	Excitation current	
M_f	Maximum mutual inductance between stator and rotor	
ψ	Product of mutual inductance and excitation current	
T_e	Induced electric torque	
P_s	Synchronverter output active power	W
P_{ref}	Reference active power	W
Q	Synchronverter output reactive power	VAR
Q_{ref}	Reference reactive power	VAR
ω_s	Rotor angular speed	rad/s
θ_s	Rotor angle	Deg
e_{abc}	Induced electromotive force	V
v_g	Grid voltage	V
v_s	Synchronverter output voltage	V
i_s	Synchronverter output current	A
L_1, L_2	Filter inductors	mH
C_f	Filter capacitor	μF
R_s	Series resistor	Ω
V_{DC}	DC bus voltage	V
V_n	Nominal phase voltage	V

S_n	Nominal power	kVA
f_{sw}	Switching frequency	kHz
f_n	Nominal frequency	Hz
f_s	Synchronverter frequency	Hz
D_f	Damping coefficient	
J	Virtual inertia	
D_v	Voltage droop coefficient	
K	Integrator gain	
τ_f	Frequency loop time constant	s
τ_v	Voltage loop time constant	s
ω_{res}	Resonance frequency	rad/s
V_d	RMS difference between v_o and v_g	V
K_f, I_f	PI gains	
K_v, I_v	PI gains	
V_{Th}	Threshold voltage	V
ω_s	Synchronizer output	rad/s
v_s	Synchronizer output	V

Chapter 1

Introduction

The consistent and swift expansion of solar photovoltaic and wind power generation capacity in the past few decades seems to be unparalleled. High rates of growth seem expected to continue, as these technologies are now available in many regions of the world at prices competitive with or lower than those of incumbent fossil fuel companies [1, 2]. Consequently, the future power grid will be a Renewable Energy Resources (RERs) dominant grid.

Renewable energy sources are natural resources or processes that can produce energy that are, by human criteria, renewable quicker than they can be utilized. Fossil fuels, such as coal, peat, oil, natural gas, and uranium ore, are replaced by renewable energy sources (RES). These are also renewable, but it takes a lot longer, and predictions indicate that they may run out quite quickly. Moreover, when they burn, carbon dioxide is released into the sky, accelerating the greenhouse effect and global warming. However, the majority of renewable energy sources are categorized as "green energy," or non-polluting, environmentally benign energy [3]. Solar energy is one of the leading RERs due to the availability of sunlight on the earth's surface, easy installation and maintenance, lack of wear and tear, quiet operation, and zero environmental pollution [4, 5].

This chapter discusses technical issues, challenges, and modern solutions related to inverter-dominated power grids. It also covers the motivation behind the research work, research objectives, and contributions to the research community.

1.1 Renewable Energy Sources and Challenges for Future Power Grid

As renewable energy sources (RERs) become more prevalent, traditional synchronous generator (SG) dominated power grids are transitioning to inverter-dominated grids, as shown in Figure 1.1. According to the statistics of year 2023 [6] China is leading the world in generating 31.7% of its electricity from photovoltaic (PV), similarly it reached upto 16% in USA, Japan's PV share is 8.4%, India is generation from PV by 6.6% and Germany ia at 4.7%. A similar trend is observed in Pakistan. The Ministry of Science and Technology in Pakistan has taken significant steps in developing PV panels over the last decade [7].

The National Institute of Silicon Technology (NIST) has developed PV modules and other infrastructure for solar power generation. In the year 2017-18, the National Transmission and Dispatch Company (NTDC) procured 400 MW from solar and 985 MW from wind Independent Power Producers (IPPs) [8]. During 2020-2021 a total of 8417 net metering licenses with the cumulative capacity of 145.881 megawatt were issued to distribution companies. Additionally, during the same period National Electric Power Regulatory Authority (NEPRA) [9] issued nineteen (19) new generation licenses with the cumulative installed capacity of 50.0264 megawatt to PV companies. The Alternative Energy Development Board (AEDB) is currently pursuing twenty-two solar power projects with a cumulative capacity of 890.80 megawatt [10]. The Quaid-e-Azam Solar Power Park in Bahawalpur is one of the largest solar power plant in Pakistan [11].

The adoption of Plug-in Hybrid Electric Vehicles (PHEVs) and Electric Vehicles (EVs) is increasing worldwide. As a result, there is a growing presence of battery

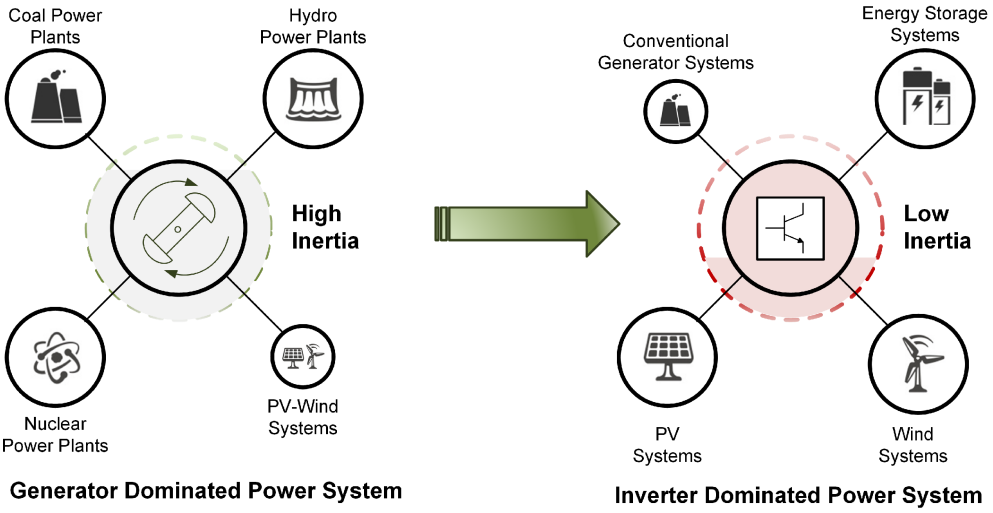

FIGURE 1.1: Future Power Grid [11]

chargers in the power grid [12]. Renewable energy resources (RERs), Energy Storage Devices (ESDs), EVs, and other technologies are connected to the grid using solid-state Power Electronic Converters (PECs). Additionally, modern loads are also connected through PECs [13]. The increasing use of these inertia-less converters in the traditional grid creates challenges for grid dynamics and stability [14]. During faults or load variations, the frequency Nadir and the Rate of change of Frequency (ROCOF) are likely to be higher due to lower rotating inertia in the power grid [15]. The frequency Nadir corresponds to the minimum value of frequency reached during the transient period before a frequency event occurs. The intermittent and non-dispatchable nature of renewable energy, along with high oscillations, also impacts grid stability. Grid stability refers to the power system's ability to return to a steady state after a disturbance. The high penetration of PV panels presents technical challenges and opportunities for power system engineers in operating the future power grid [16].

Grid disturbances such as short circuits, voltage sags, dips, and frequency changes due to frequent switching of heavy loads and generation units interact with the PECs, further increasing complexity and uncertainty in operating conditions [17]. The decreasing inertia of the power system, stemming from the integration of more PV panels into the power grid, poses a major threat to frequency stability

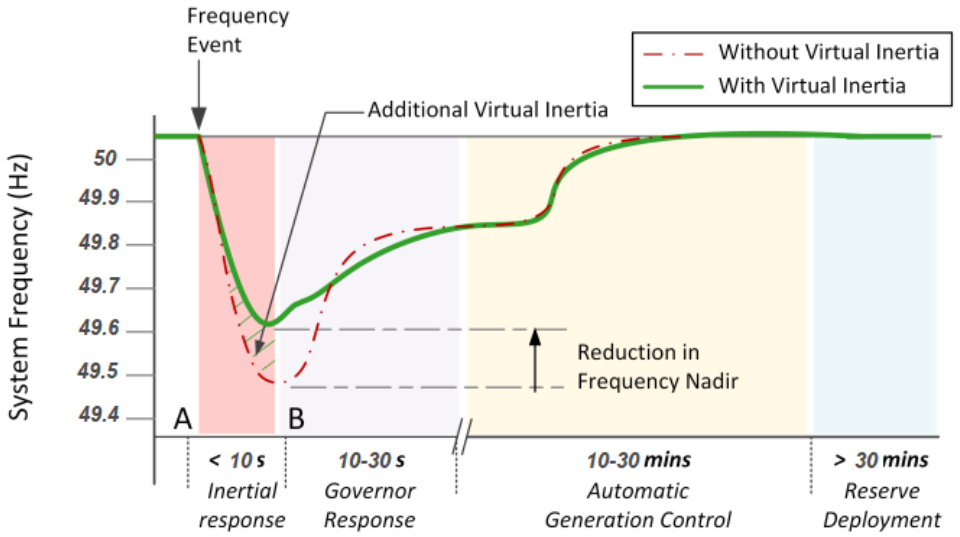

FIGURE 1.2: Significance of virtual inertia[11]

[18]. Currently, the trend in integrating PV panels involves tracking the Maximum Power Point (MPP) and injecting the maximum power into the grid. This approach is suitable only when PECs represent a small share of the overall grid capacity. However, with renewable energy resources expected to supply a significant portion of the grid's capacity in the future, the casual behavior of PECs will no longer be acceptable [19].

1.2 The Significance of Virtual Inertia

The power grid is transitioning towards an inverter-dominated system, which is leading to a reduction in the rotation inertia of the power system. This reduced inertia results in a lower frequency Nadir and a higher rate of change of frequency (ROCOF), which can cause frequency relays to trip and potentially lead to blackouts [20]. To address this issue, it is necessary to incorporate virtual inertia in power electronic converters (PECs) to enhance system stability and facilitate the integration of the renewable energy resources (RERs) in future power networks.

Figure1.2 illustrates the transient response of the power system following a frequency event, showing that the frequency Nadir of the system without virtual inertia is lower compared to the system with virtual inertia, and the ROCOF is

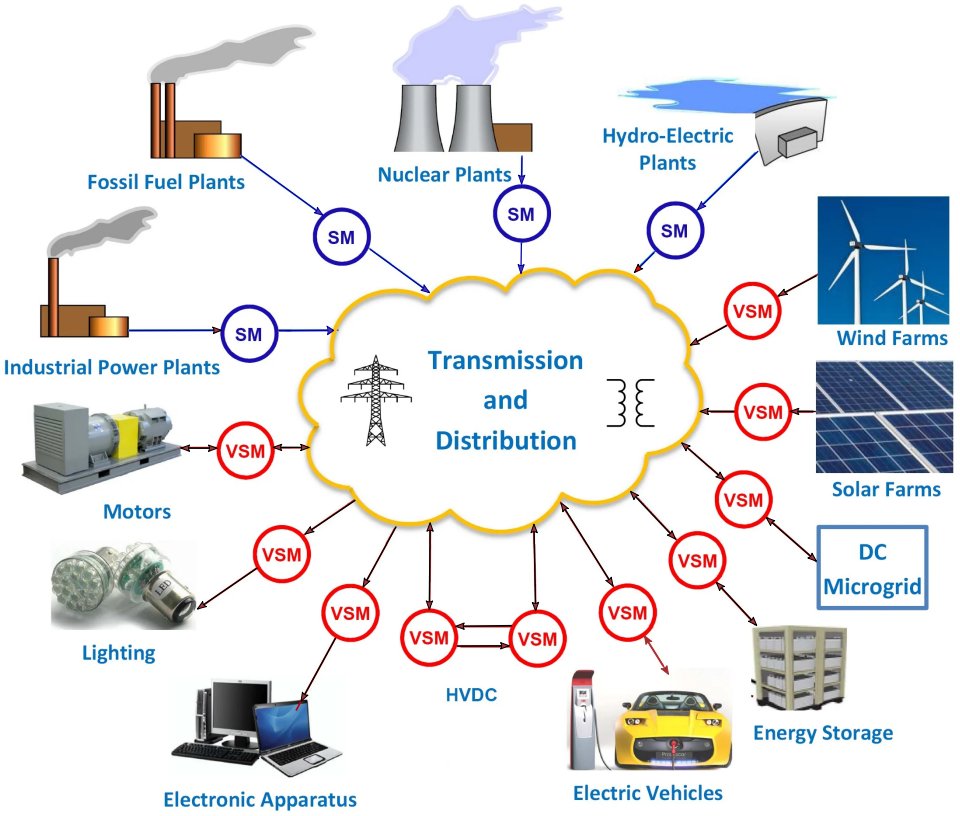

FIGURE 1.3: VSM dominated future power grid [21]

higher in the system without virtual inertia. To incorporate virtual inertia in inverter-dominated power grids, researchers have proposed the idea of replicating essential features of synchronous machines in PECs. These PECs, referred to as Virtual Synchronous Machines (VSMs), behave like synchronous machines and provide support to the grid during frequency and voltage events[21]. Although these units are physically inverters, their behavior resembles that of synchronous machines.

With the use of VSMs, the future power grid can be depicted as shown in Figure 1.3.

1.3 Virtual Synchronous Machines (VSMs)

The virtual synchronous machine can function as a virtual synchronous motor or a virtual synchronous generator, depending upon the direction of exchange of energy

between the converter and the grid [22]. When the Power Electronic Converter (PEC) is operating as a rectifier, it behaves like a synchronous motor, and when it operates as an inverter, it behaves like a synchronous generator. Many VSM topologies incorporate a comprehensive mathematical model of SM [23]. These topologies include the IEPE's topology, VISMA, KHI Lab's topology [24] and Synchronverter [19]. Mathematical modeling offers various advantages over real SMs, as the parameter values are not constrained by the physical design. A wide range of parameter values can be used in virtual machines that may not be feasible in real machines. These parameters can also be modified during operation, unlike real machines [25]. Furthermore, the losses associated with virtual machine impedances are not actual losses and are sent back to the dc bus, thus having no effect on system efficiency [19]. Another implementation of VSM involves the application of rotor swing equation in real SMs, while ignoring detailed mathematical modeling. Ise Lab's VSM [21] is a well-known example following this concept. Other well-known topologies, including Virtual Synchronous Generator (VSG) [21], Synchronous Power Controller (SPC) [26], and Virtual Synchronous Controller (VSYNC) [27], model the power balance relations of real SMs and simulate inertia. The classification of different VSM topologies is shown in Figure1.4.

1.4 Introduction to Synchronverter

Out of all the VSMs proposed, synchronverter is accepted as the best replication of a synchronous generator in terms of its performance and simple design [19]. Similar to synchronous generators, the synchronverter has the virtual inertia which helps to keep it synchronized with the power grid without requiring a dedicated synchronization device [28]. It can operate in grid-connected and stand-alone mode without any changes to the circuit of its controller. Additionally, it supports system voltage and frequency, especially in weak grids [29]. A weak grid is defined as a power grid with a low inertia and low short-circuit ratio. The synchronverter can mimic all essential features of a synchronous machine that are necessary for power grids of the future [19]. Similar to a synchronous generator, careful attention

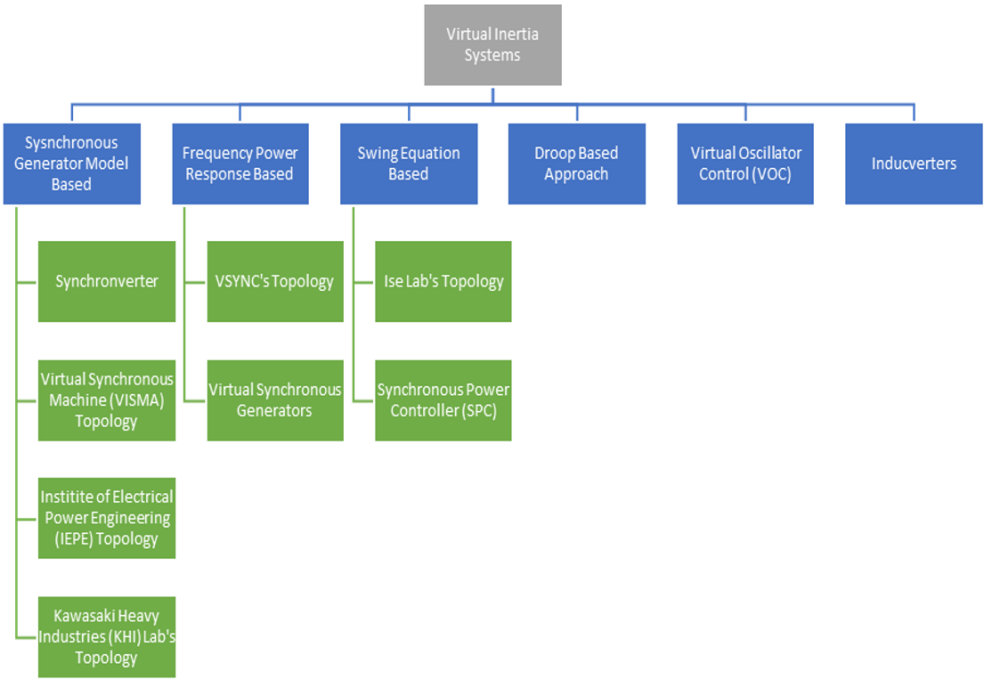

FIGURE 1.4: VSM Topologies [21]

is needed for the initial synchronization of the synchronverter with the power grid to prevent high current and power transients at grid connection. The primary focus of this research is on the initial synchronization of a synchronverter with an unbalanced grid which has a steady state unbalance among its voltages.

1.5 Motivation

As discussed in section1.1, the penetration of Renewable Energy Resources (RERs) is increasing in power grids worldwide, including Pakistan. This trend of installing more RERs is leading to power grids being dominated by conventional inverters. These inertia-less Power Electronic Converters (PECs) are needed to mimic synchronous generators to support frequency and voltage in the future power grid. One of the Virtual Synchronous Machines, known as the Synchronverter, provides both frequency and voltage support to the grid. Although literature [19] claims the synchronverter to be the best replication of a synchronous generator, there is always room for improvement. The synchronverter can stay connected with the grid without a need of a dedicated synchronization unit but it requires

a pre-synchronizer for its initial synchronization. For this purpose, the PLL-Less schemes are more popular than PLL-based schemes due higher complexity and uncertainty during harsh grid conditions. Most of the PLL-Less schemes having hot-seamless capability are proposed for balanced grid only. Therefore, a PLL-Less scheme is needed for hot-seamless initial synchronization of synchronverter with an unbalanced grid which is not available in literature.

1.6 Objectives of the Research

In order to incorporate renewable energy resources (RERs) into the future power grid, virtual synchronous machines (VSMs) are a preferable option over inertia-less power electronic converters (PECs). This research seeks to improve the performance of the pre-synchronization of synchronverters when integrating with an unbalanced power grid. The main objectives of this research are as follows:

1. Enhance the existing Fourier Analysis-based PLL-Less self-synchronizer to improve the pre-synchronization of the synchronverter with an unbalanced grid, ensuring uninterrupted power supply to local loads during the pre-synchronization process.

2. Evaluate and compare the performance of enhanced pre-synchronizer with the existing Fourier Analysis-based PLL-Less self-synchronizer.

1.7 Research Contribution

The main contributions of this research work is as follows:

- An instantaneous positive sequence extraction block is embedded in an existing FA-based PLL-Less self-synchronizer for achieving hot-seamless pre-synchronization of synchronverter with an unbalanced grid.

1.8 Thesis Organization

The structure of upcoming chapters is as follows:

Chapter 2 covers the literature review of synchronverter. It includes derivation of the mathematical model of synchronverter, its pre-synchronization techniques with balanced and unbalanced grid. The application potential of synchronverter is also discussed. Based on the outcome of review a gap analysis and problem statement are formulated. Research methodology and technique used in work is also presented. Finally addressed the applications of proposed scheme.

In Chapter 3, a brief introduction to the existing FA-based PLL-Less self synchronizer and its limitations against its usage with unbalanced grid is given. Further the implementation of extracting instantaneous symmetrical components of an unbalanced grid is discussed. Finally, a modification in existing pre-synchronization scheme is presented.

In Chapter 4, the simulation of synchronverter with enhanced pre-synchronizer is done out in MATLAB/Simulink in different scenarios of grid. The results of existing and enhanced schemes are compared to evaluate the proposed enhanced pre-synchronizer.

Conclusions is given in Chapter 5 and the future directions are also discussed for encouragement of research in this field.

Chapter 2

Literature Review

Over the past decade, researchers have proposed various Virtual Synchronous Machine (VSM) topologies. Each of these topologies has different practical implementations and advantages.

The Synchronverter is proved to be the best replica of a synchronous machine because it represents the same dynamics from the grid's point of view [19]. This topology has been well developed and validated in various applications in literature [30]. The upcoming sections will provide a review of literature related to the Synchronverter.

This chapter presents a literature review that will be used to identify research gaps and formulate the problem statement. Finally, the methodology used in this research and its potential applications in the power grid will be discussed at the end of this chapter.

2.1 Mathematical Model of Synchronverter

In the literature, mathematical model of the synchronous machine (SM) is found in [31, 32]. [19] considers a two-pole round-rotor synchronous machine for the synchronverter, which is also followed in this study. For simplicity, losses of core

and the friction losses are not considered in the design. Additionally, balance conditions with a positive phase sequence are assumed. The variation in the rotor and stator inductances due to position of rotor are ignored. Furthermore, in this study, the damper winding is not taken into account .

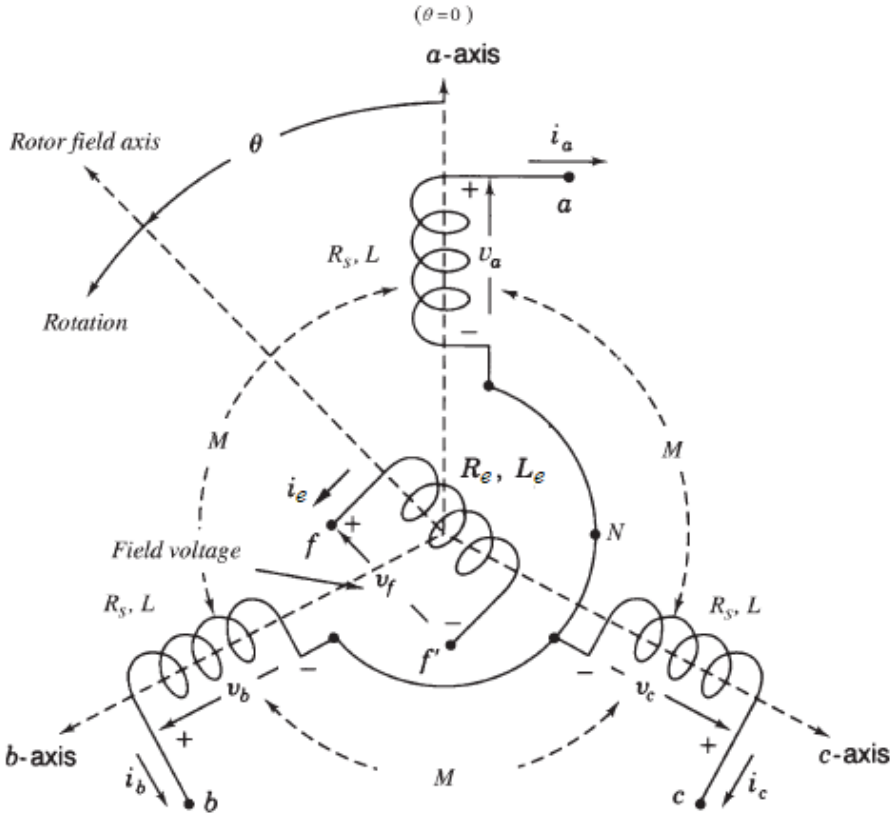

FIGURE 2.1: Winding of Synchronous Machine [19]

In Figure 2.1 the winding structure of a synchronous machine is illustrated. The stator winding consists of coils with self inductance L_s, resistance R_s and the mutual inductance M. The self-inductance and resistance of the rotor excitation coil is designated by L_f and R_f respectively. The mutual inductance between rotor and stator excitation coils is a function of its rotor angle θ_f and be defined as:

$$\begin{aligned} M_{af} &= M_f \cos(\theta_f) \\ M_{bf} &= M_f \cos(\theta_f - \frac{2\pi}{3}) \\ M_{cf} &= M_f \cos(\theta_f - \frac{4\pi}{3}) \end{aligned} \tag{2.1}$$

The flux linkages of stator is expressed as:

$$\begin{aligned}\phi_a &= Li_a - Mi_c - Mi_b + M_{af}i_f \\ \phi_b &= Li_b - Mi_c - Mi_a + M_{bf}i_f \\ \phi_c &= Li_{sc} - Mi_b - Mi_a + M_{cf}i_f\end{aligned} \tag{2.2}$$

Where i_a, i_b, and i_c denote the phase current in stator winding and i_f is field excitation current in the rotor winding.

Since the conditions are assumed to be balanced, the following equation holds because a neutral is absent:

$$i_a + i_b + i_c = 0. \tag{2.3}$$

When the neutral is present, the sum of the three phase currents equals to i_n. Since the design process assumes a balanced condition, the neutral current is also assumed to be 0. By using Equations 2.1 to 2.3, we can simplify the stator flux linkages as:

$$\begin{aligned}\phi_a &= (L+M)i_a + M_f i_f \cos(\theta_s) \\ \phi_b &= (L+M)i_b + M_f i_f \cos(\theta_s - \frac{2\pi}{3}) \\ \phi_c &= (L+M)i_c + M_f i_f \cos(\theta_s - \frac{4\pi}{3})\end{aligned} \tag{2.4}$$

Simplifying the Equation 2.4 yields:

$$\begin{bmatrix}\phi_a \\ \phi_b \\ \phi_c\end{bmatrix} = (L+M)\begin{bmatrix}i_a \\ i_b \\ i_c\end{bmatrix} + M_f i_f \begin{bmatrix}\cos\theta_s \\ \cos(\theta_s - \frac{2\pi}{3}) \\ \cos(\theta_s - \frac{4\pi}{3})\end{bmatrix} \tag{2.5}$$

For simplification, let $L + M = L_s$, and the flux linkages of stator equal to Φ_s as:

$$\Phi_s = \begin{bmatrix}\phi_a \\ \phi_b \\ \phi_c\end{bmatrix} \tag{2.6}$$

Let stator currents are designated by i_s as:

$$i_s = \begin{bmatrix} i_a \\ i_b \\ i_c \end{bmatrix} \tag{2.7}$$

Also, let:

$$\widetilde{\cos}\theta_s = \begin{bmatrix} \cos\theta_s \\ \cos(\theta_s - \frac{2\pi}{3}) \\ \cos(\theta_s - \frac{4\pi}{3}) \end{bmatrix} \tag{2.8}$$

The equation 2.4 can be expressed as:

$$\Phi_s = L_s i_s + M i_f \widetilde{\cos}\theta_s \tag{2.9}$$

The rotor flux linkage is expressed as.

$$\Phi_f = L_f i_f + M_{af} i_a + M_{bf} i_b + M_{cf} i_c \tag{2.10}$$

Using the mutual inductance values from Equation 2.1 to simplify the rotor flux linkage yields:

$$\begin{aligned} \Phi_f &= L_f i_f + M\cos(\theta_s) i_a + M\cos(\theta_s - \frac{2\pi}{3}) i_b + M\cos(\theta_s - \frac{4\pi}{3}) i_c \\ &= L_f i_f + M \begin{bmatrix} i_a \\ i_b \\ i_c \end{bmatrix}^T \begin{bmatrix} \cos\theta \\ \cos(\theta_s - \frac{2\pi}{3}) \\ \cos(\theta_s - \frac{4\pi}{3}) \end{bmatrix} \end{aligned} \tag{2.11}$$

The rotor flux linkage found in the previous equation can be expressed as follows with additional simplification.

$$\Phi_f = L_f i_f + M \langle i_s, \widetilde{\cos}\theta_s \rangle \tag{2.12}$$

Where, $\langle i_s, \widetilde{\cos}\theta_s \rangle$ is the usual dot product of the stator current i_s and $\widetilde{\cos}\theta_s$ in the real numbers domain.

The rate of change of flux in stator can be written as:

$$\left.\frac{d\Phi_s}{dt}\right|_{i_s,i_f\text{constant}} = -\dot{\theta}_s M i_f \widetilde{\sin}\theta_s \tag{2.13}$$

An electromotive force is induced by the rate at which stator flux changes in stator coils and can be expressed by Lenz's Law as [32]:

$$\begin{aligned} e &= -\frac{d\Phi_s}{dt} \\ &= \dot{\theta}_s M i_f \widetilde{\sin}\theta_s \end{aligned} \tag{2.14}$$

Where, $\dot{\theta} = \omega$ in radians per second is the angular speed of synchronous machine's rotor.

Energy that is stored in the magnetic field of synchronous machine can be expressed as.

$$\begin{aligned} E &= \frac{1}{2}\langle i_s, \Phi_s\rangle + \frac{1}{2} i_f \Phi_f \\ &= \frac{1}{2}\langle i_s, L_s i_s + M_f i_f \widetilde{\cos}\theta_s\rangle + \frac{1}{2} i_f (L_f i_f + M_f \langle i_s, \widetilde{\cos}\theta_s\rangle) \\ &= \frac{1}{2}\langle i_s, L_s i_s\rangle + \frac{1}{2} M_f i_f \langle i_s, \widetilde{\cos}\theta_s\rangle + \frac{1}{2} L_f i_f^2 + \frac{1}{2} M_f i_f \langle i_s, \widetilde{\cos}\theta_s\rangle \\ &= \frac{1}{2}\langle i_s, L_s i_s\rangle + \frac{1}{2} L_f i_f^2 + M_f i_f \langle i_s, \widetilde{\cos}\theta_s\rangle \end{aligned} \tag{2.15}$$

By measuring the rate at which the stored energy in the magnetic field changes in relation to the rotor rotation, one may determine the induced electric torque of the synchronous machine. [33].

$$T_e = -\frac{\partial E}{\partial \theta_s} = M_f i_f \left\langle i_s, \widetilde{\sin}\theta_s \right\rangle \tag{2.16}$$

The induced electric torque obtained form above equation can be used to calculate the active power P produced by the synchronous machine and angular speed of rotor can be calculated as follows [32]:

$$P = \omega T_e = \dot{\theta}_s M_f i_f \left\langle i_s, \widetilde{\sin}\theta_s \right\rangle \tag{2.17}$$

and the reactive power Q is written as.

$$Q = \dot{\theta}_s M_f i_f \left\langle i_s, \widetilde{\sin}(\theta_s - \frac{\pi}{2}) \right\rangle = -\dot{\theta}_s M_f i_f \left\langle i_s, \widetilde{\cos}\theta_s \right\rangle \tag{2.18}$$

For simplification of the Equations 2.14, 2.16 and 2.18, the product of maximum value of mutual inductance between rotor and stator excitation coils and the field excitation current can be supposed as $M_f i_f = \psi$. This gives:

$$e_{abc} = \omega_s \ \psi \ \widetilde{\sin}\theta_s \tag{2.19}$$

$$T_e = \psi \left\langle i_s, \widetilde{\sin}\theta_s \right\rangle \tag{2.20}$$

$$Q = -\omega_s \psi \left\langle i_s, \widetilde{\cos}\theta_s \right\rangle \tag{2.21}$$

Where, ω is the angular speed of rotor (radians per second). Hence the synchronverter model is based on Equations 2.19 to 2.21.

2.2 Modification in the Original Synchronverter

Numerous changes to the original synchronverter have been described in the literature as improvements. Table 2.1 shows the summary of some modifications. In [34], a self-synchronized synchronverter is presented to allow synchronverter initial synchronization with grid independent of Phase-Locked Loop (PLL). A feature of regulating DC bus voltage is added in original synchronverter in [35].

Five modifications are proposed in original synchronverter to improve its stability and dynamic performance in [36]. These modifications included field current control, addition of virtual losses in power formulas, and addition of virtual inductor and virtual capacitor in original synchronverter.

[37] proposes a fault riding through capability in which a synchronverter's control shifts to hysteresis mode to reduce the inrush currents during faults while supplying the grid with the necessary amount of real and reactive power. Single-phase counterpart of synchronverter is presented in [38] for residential roof-top DGs.[39]

proposes a modification in original synchronverter to keep its output voltage and frequency within specified ranges. It also added the capability of riding-through a fault during unsymmetrical grid faults.

For improving the performance of synchronverter with unbalanced grid a resonant controller based synchronverter has been designed in [40]. References [41, 45] adjusted the transient response speed of synchronverter without affecting steady-state performance by using damping correction loop. In [42] the model of damping winding of synchronous machine is included in original synchronverter for attenuation of oscillations in power grid. A fault tolerant synchronverter has been developed in [43]. An improvement has been done in [44] to reduce the harmonic distortion in grid current due to voltage amplitude measurement errors in original synchronverter.

2.3 Synchronization with the Grid

The synchronverter is capable of staying synchronized with the grid without a requirement of a separate synchronization unit. It can seamlessly do transition from grid connected to standalone mode not requiring adjustments to the controller. However, it does require a pre-synchronizer to monitor the frequency and phase of the power grid as a reference prior to grid connection [46] [38].

The operational modes of the synchronverter and the transition between them is shown in Figure 2.2. It is clear from this figure that a separate synchronization unit is only needed for its initial synchronization with the grid. Several PLL-Less techniques have been developed by researchers for pre-synchronization of the synchronverter.

Most of these schemes are designed by considering an ideally balanced grid while relatively a little work has been done for pre-synchronization with an unbalanced grid. Moreover a synchronization scheme must posses a hot-seamless capability in such applications where critical loads are present.

TABLE 2.1: Summary of modification in synchronverter

Modifications	**Year**	**Details**	**References**
Self-synchronization using virtual impedance	2014	Proposes self-synchronization without PLL using virtual current instead of actual grid current	[34]
Voltage regulation of DC-Bus	2014	Proposed bidirectional with regulation of DC bus voltage. It also embedded fault-ride-through capability in synchronverter.	[35]
Virtual Capacitor and Virtual Inductor in original synchronverter	2017	Proposed virtual capacitor, virtual inductor and current controller for improved dynamic performance and stability of synchronverter	[36]
Controller Mode switching	2017	Protection against the transient currents from synchronverter during grid faults	[37]
Single-phase Synchronverter design	2018	Designed a single phase synchronverter having PLL-Less initial synchronization capability	[38]
Bounded Voltage and Frequency	2018	Proposed scheme for keeping Voltage and Frequency of synchronverter within limits	[39]
Resonant controller based synchronverter	2019	A resonant controller embedded in synchronverter for improving its response with unbalanced grid	[40]
Decoupled response	2022	Decoupled response for inertia from the regulation of primary frequency	[41]
Virtual damper winding	2022	Attenuation of power system oscillations	[42]
Current-Controlled Synchronverter	2023	A Grid Fault Tolerant Grid Forming Inverter	[43]
Fast Current Loops	2023	Reduces the harmonic distortion and fluctuation in amplitude of the grid-side currents that produces due to grid voltage measurement errors	[44]

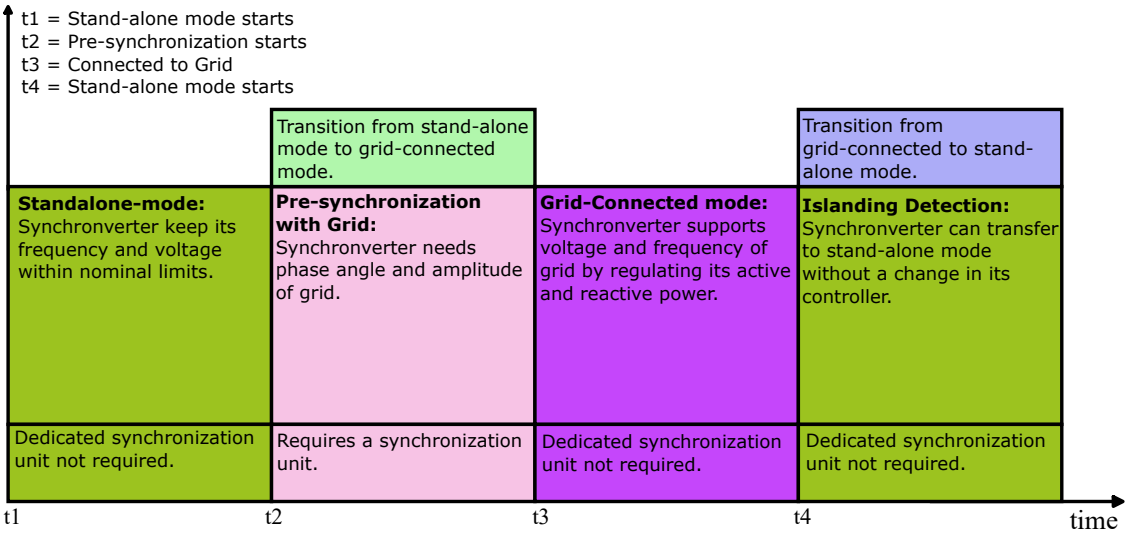

FIGURE 2.2: Synchronverter operation modes [47]

Hot-seamless capability defines that the supply to critical loads like hospital or military installations must not be interrupted during pre-synchronization process. A few PLL-Less schemes has been reported in literature [46],[38] which can achieve hot-seamless synchronization with a balanced grid but no PLL-Less scheme is designed with hot-seamless capability for unbalanced grid situation.

The strategies designed for initial synchronization of synchronverter with a balanced and unbalanced power grid are reviewed in this section. Table 2.2 and 2.3 shows the comparison among synchronization systems designed for balanced and unbalanced grid respectively.

2.3.1 Pre-synchronization with a Balanced Grid

A balanced grid is a three-phase power system where the following conditions are met:

1. Voltage Magnitude: The magnitude of voltage for all three phases is same.
2. Phase difference: The phase angle is 120 degrees between any two phases.
3. Currents: The magnitude of current is equal in each phase.

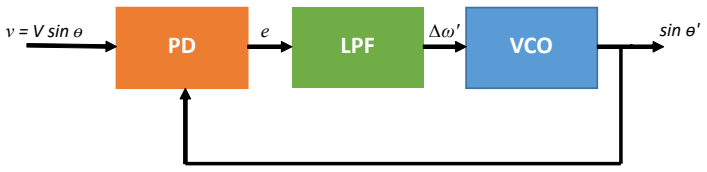

FIGURE 2.3: Basic Block diagram of PLL

This ideal condition ensures reduced losses, efficient power transfer and minimal equipment stress.

The schemes proposed in literature for pre-synchronization of synchronverter with a balanced grid are briefly explained in following sub-section.

2.3.1.1 PLL-Based Synchronizer [19]

Initially the Phase-locked loop (PLL) was used for the pre-synchronization of the synchronverter in [19]. Later on, same technique was used in [48–50] to achieve PLL-based initial synchronization with a balanced grid.

As shown in Figure 2.3 a basic PLL consist of a control loop having a phase detector, a low pass filter and a voltage controlled oscillator for estimation of phase angle of the signal. It can additionally provide the frequency but cannot give any information on amplitude of the signal.

When PLL is utilized extensively in the electrical grid, it has some limitations and downsides, which are discussed below:

- Multiple PLLs operating in parallel contend with each other and can cause loss of synchronism, instability and increased complexity. [51].
- Tuning of the PLL parameters is quite difficult for achieving an adequate performance [52].

- The Voltage Controlled Oscillator (VCO) can affect the stability and performance of PLL as it is very sensitive to noise, switching transient and frequency and voltage variations. [53].

- PLL reduces the performance of PEC owing to the existence of steady-state errors, frequency changes and voltage sags, harmonic distortions, specifically when PEC is linked to a weak grid [54].

Due to the above-mentioned drawbacks, PLL-less synchronization approaches are being addressed in literature. The upcoming section presents an overview of PLL-Less self synchronizing schemes.

2.3.1.2 Virtual Current Based Self-synchronizer [34]

First PLL-less self-synchronization approach for pre-synchronization of synchronverter is proposed in [34]. Same approach is implemented for a wind farm integration into grid in [55] for a single phase PV synchronverter in [56], for parallel operation of synchronverters in [57], and for droop based controller in [58]. As shown in Figure 2.4, this is a virtual impedance based self-synchronization approach introduced in original synchronverter. During the process of pre-synchronization instead of actual grid current, a virtual current is fed to the synchronverter control. This virtual current can be represented as:

$$i_s = (\frac{1}{Ls + R})(e_{abc} - v_g) \tag{2.22}$$

Where e is the induced machine electromotive force, defined in Eq. 2.14, v_g is grid voltage and R and L are the virtual resistor and virtual inductor respectively. During synchronization process, the references of active and reactive power are set to 0 and frequency and voltage droops are disabled. Synchronization is achieved when the virtual current and $e - v_g$ become zero. A PI controller is used in frequency droop loop this to regulate the output of damping coefficient block and generate a new reference frequency.

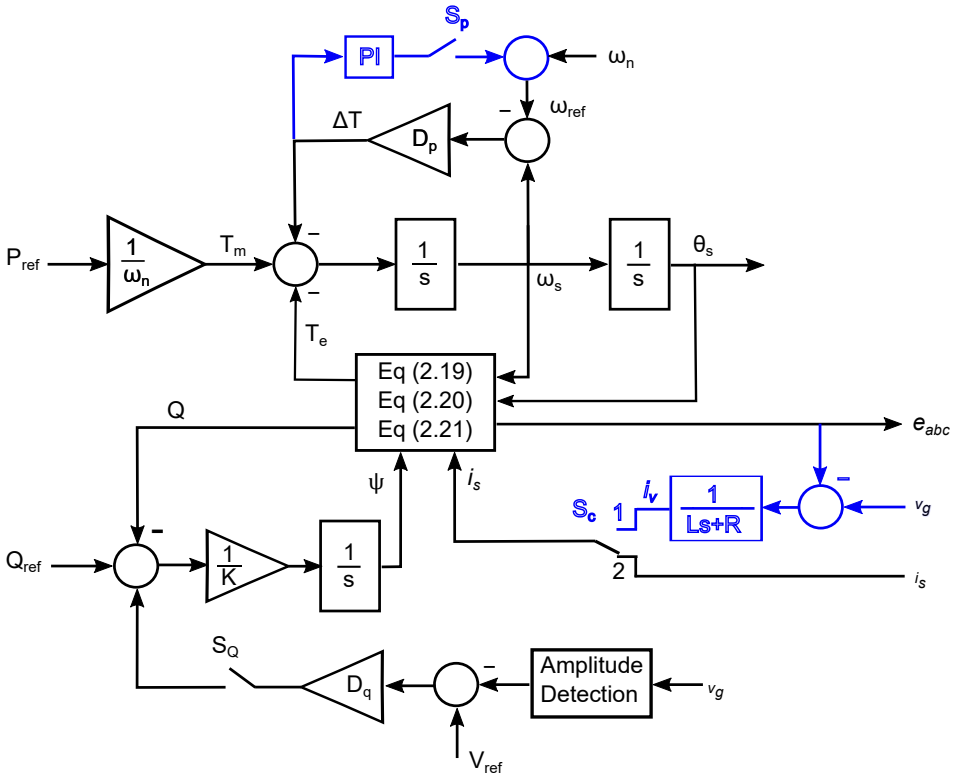

FIGURE 2.4: Block Diagram of Virtual impedance based self-synchronizer [34]

Despite being the most widely used PLL-less pre-synchronization method among researchers, it has few drawbacks, which are discussed in the following lines:

- This approach maintains zero reference active and reactive powers and feeds the synchronverter with virtual current during the synchronization process rather than real grid current. Therefore the synchronverter cannot provide power during the synchronization process [38, 46]. This implies that when switching from stand-alone to grid-connected mode, the local load needs to be disconnected from the output. When there is a critical local load coupled to the synchronverter output, this kind of synchronization technique is not appropriate.

  A hospital, data center, military installation, or intelligence center that needs continuous electrical power is considered a critical load.

- Virtual inductance and resistance must be precisely tuned for virtual impedance-based self-synchronization. Higher i_v leads to quicker synchronization when L and R are smaller. On the other hand, oscillations in frequency may

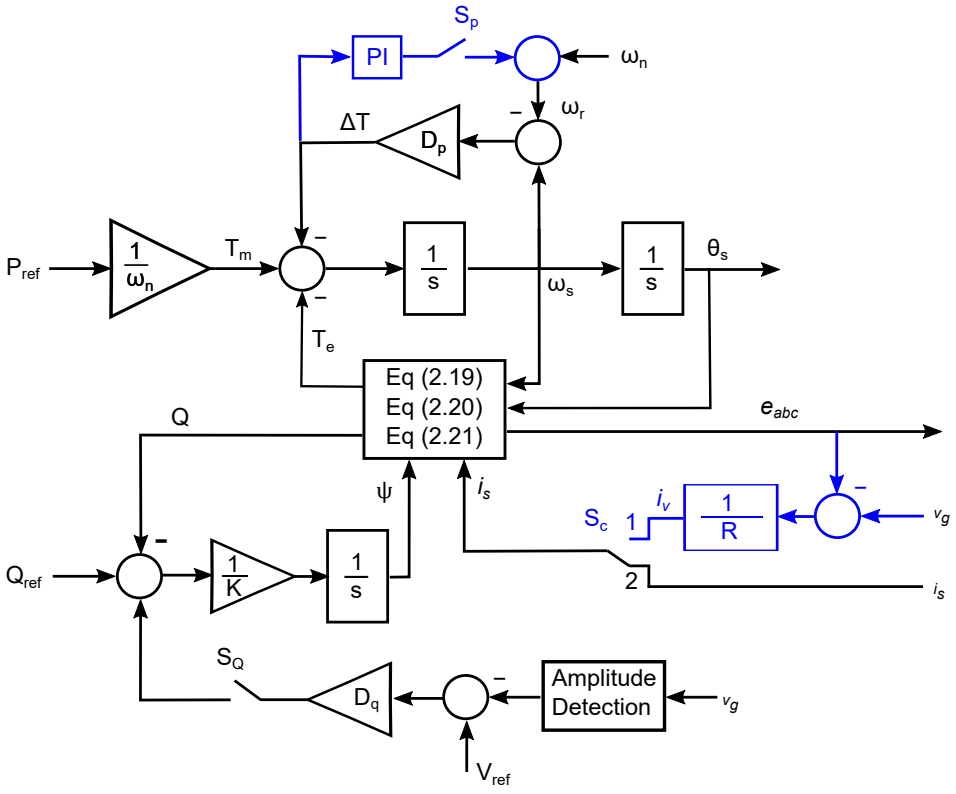

FIGURE 2.5: Block Diagram of Virtual resistance-based self-synchronizer [60]

arise from very small quantities [34]. Unstable eigenvalues caused by virtual inductance L can result in synchronization failure and uncertainties [59].

A self-synchronized synchronverter should appropriately handle these two constraints.

2.3.1.3 Virtual Resistance Based Synchronization [60]

This method uses a virtual resistance for initial synchronization of synchronverter rather than a virtual impedance [60]. This eliminates the unstable eigenvalues generated by virtual inductance in [34].

Figure 2.5 shows the schematic diagram of the virtual resistance-based self-synchronization technique.

When compared to virtual impedance, this method produces a lower virtual current peak. Nevertheless, this approach has several limitations covered in the following points.

- When employing virtual resistance based self-synchronization, a transformation of coordinate with rotational matrices must be performed [30]. The controller has to do extensive calculations as a result of this modification in result the computational burden is increased.

- Similar to the virtual current approach, during synchronization process, the virtual current is used instead of actual grid current and the real and reactive power references are set to zero. Therefore this approach also unable to provide continuous power to critical local load during synchronization process.

2.3.1.4 Differential RMS Voltage Based Self-synchronizer [38]

This method addresses the synchronverter's seamless transfer capacity during the synchronization process after realizing the significance of the hot-seamless capability required for the essential load [38].

This approach uses a PI controller to reduce the Root Mean Square (RMS) value of the voltage difference between the synchronverter and the grid in order to achieve pre-synchronization. The schematic diagram for this method is displayed in Figure 2.6.

The DRMSV based synchronization approach added the feature of hot-seamless transfer in synchronverter during pre-synchronization process. However, this approach has unwanted uncertainties and lags that are given below:

- This approach causes unwanted delays if the synchronverter voltage lags behind the grid voltage.

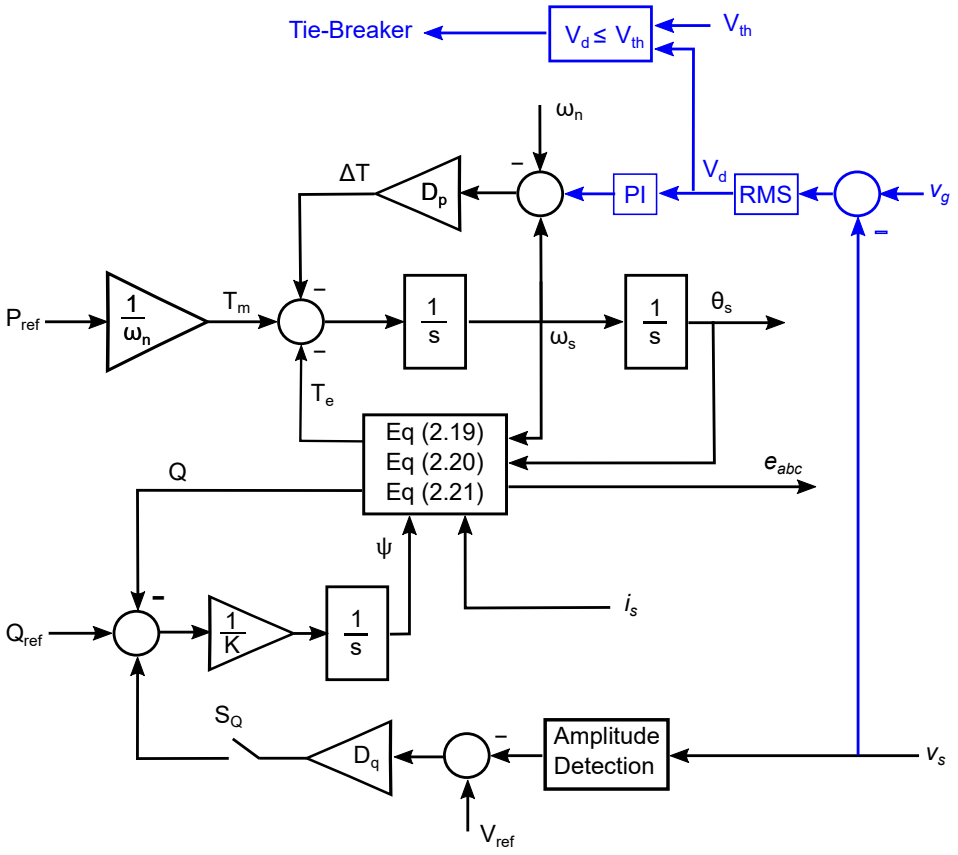

FIGURE 2.6: Block Diagram of Differential RMS Voltage Based Self-synchronizer [38]

- During pre-synchronization process, this approach always slowed down the virtual rotor speed of the synchronverter.
- This scheme cannot archive synchronization when magnitude of difference between grid and synchronverter voltages is larger than V_{Th}.

2.3.1.5 Fourier Analysis Based Self-synchronizer [46]

This approach has been developed to overcome the limitations of Differential RMS Voltage Based Synchronization (DRMSV) method. It is motivated by the fourier Series. Figure1.2 shows the block diagram of proposed synchronizer. In this scheme the grid phase angle θ_g is measured by doing the fourier analysis of grid voltage v_{ga}. During synchronization process, depending upon the magnitude and sign of the phase difference between v_{sa} and v_{ga}, the synchronverter's angular frequency ω_{syn} and voltage v_s are adjusted by respective PI controllers. The process

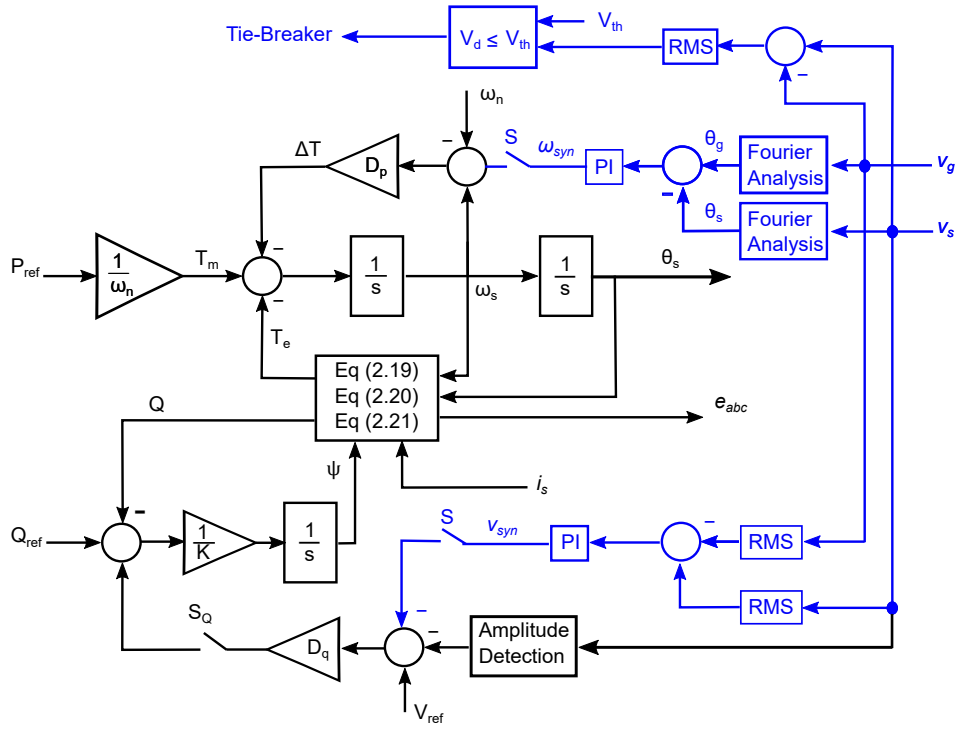

FIGURE 2.7: Block Diagram of Fourier Analysis based PLL-Less self-synchronizer [46]

continues until the rms difference between v_{sa} and v_{ga} reaches the threshold value i.e. 12V. This scheme can continue power to local load during pre-synchronization process hence it has the hot-seamless capability.

Limitations of this scheme are discussed in following points.

- If there is an unbalance in grid voltage, this approach causes high inrush currents when PCC breaker is closed.

2.3.2 Pre-synchronization with an Unbalanced Grid

An unbalanced grid is a three-phase power system where one or more of the conditions for a balanced grid are not met. This can occur due to unequal loads, faults, or other disturbances in the system. Common characteristics of an unbalanced grid include:

TABLE 2.2: Comparison of pre-synchronization techniques of synchronverter for a balanced grid

Technique	**Reference**	**Hot-Seamless Capability**	**PLL**
Phase-Locked Loop based synchronizer	[19]	Yes	Yes
Virtual Impedance based self-synchronizer	[34]	No	No
Virtual Resistance based self-synchronizer	[59, 60]	No	No
DRMSV-Based self-synchronizer	[38]	Yes	No
Fourier Analysis-Based self-synchronizer	[46]	Yes	No

1. Voltage Magnitude: The magnitudes of the voltages in the three phases are not same.

2. Currents: Current flowing through the three phases is not equal in magnitude.

3. Phase angle: The phase angle between any two phases is not 120 degrees.

The schemes proposed in literature for pre-synchronization of synchronverter with an unbalanced grid are briefly explained in following sub-section.

2.3.2.1 Positive Sequence Based Self-synchronizer [61]

In this approach the virtual impedance method [34] has been modified to achieve pre-synchronization with an unbalanced grid. During synchronization process, the virtual current that helps the synchronverter in achieving pre-synchronization with the power grid is calculated using the instantaneous positive sequences of the

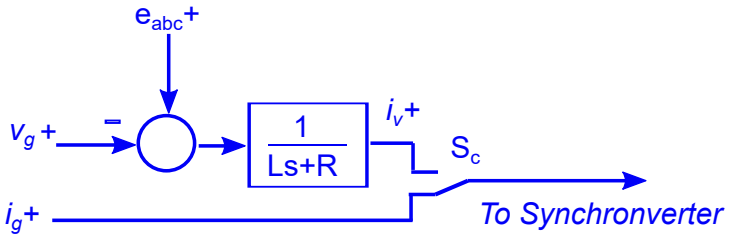

FIGURE 2.8: Virtual current calculation using positive sequences.[61]

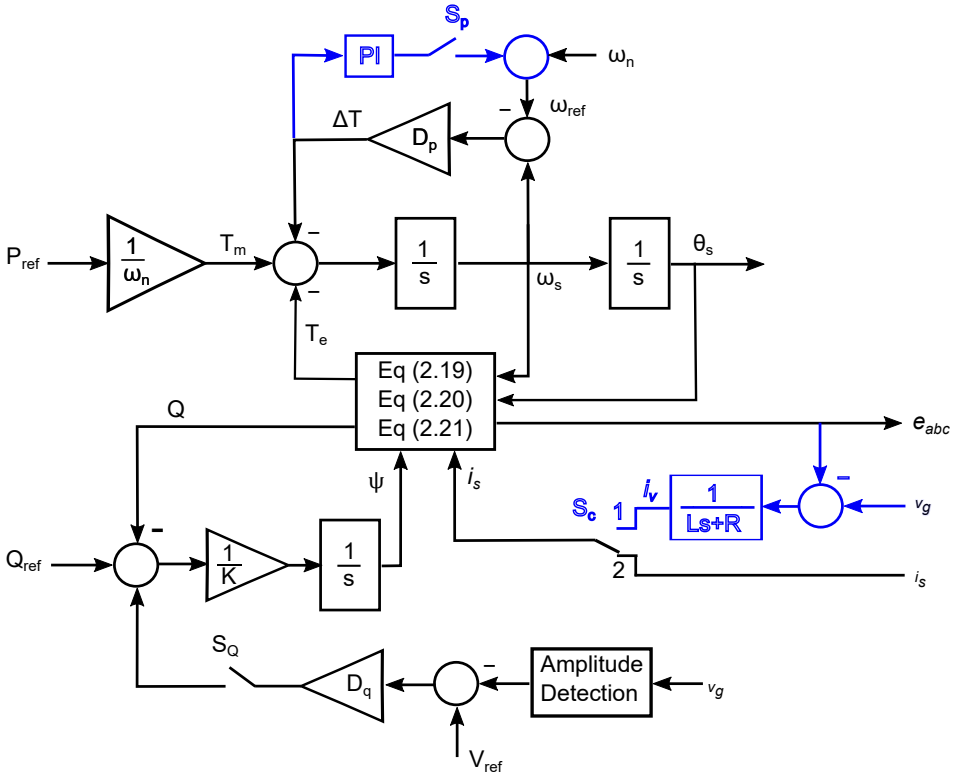

FIGURE 2.9: Block Diagram of Virtual current based self-synchronizer [61]

grid and the synchronverter voltage. The instantaneous positive sequences are extracted using Fortescue [62] and Lyon transformation [63]. This scheme can achieve synchronization regardless of balanced or unbalanced power grid. The modified part in shown in Figure 2.8 and block diagram in Figure 2.9.

The limitations of this scheme is mentioned in following points.

- This scheme is based on virtual current method [34] therefore lacks hot-seamless capability.
- The negative sequence components of grid are not compensated therefore double frequency oscillation in power and current is not eliminated.

2.3.2.2 Enhanced PLL Based Synchronizer [64]

This is a Phase locked loop (PLL) based scheme. In this scheme, an enhanced Phase locked loop (EPLL) consisting of positive, negative and zero sequence controllers is integrated into standard synchronverter. The symmetrical components of unbalanced power grid are calculated through Fortescue [62] and Lyon transformation [63]. In case of a balanced grid the negative and zero sequence parts can be discarded.

This scheme can achieve a seamless synchronization with an balanced grid with an additional feature of reducing the double frequency oscillation in injected power. The block diagram is shown in Figure 2.10.

The limitations of this scheme is mentioned in following points.

- In this method, the improved PLL requires greater amounts of computation and control loops than a standard PLL. This may increase the complexity in implementation and tuning.
- The number of control loops are more than a standard PLL. which will also increase the complexity of the system's design.
- The careful tuning of PLL is a difficult task depending upon the specific characteristics of grid and the controller can become unstable under severe unbalanced grid conditions.

2.3.2.3 Positive-Negative Sequence Based Self-synchronizer [65]

To enhance the converter's behavior under both unbalanced grid voltages and unbalanced voltage sags, this technique divides the power control into positive and negative sequence components. The instantaneous positive and negative sequences are extracted using Fortescue [62] and Lyon transformation [63].

This scheme can achieve synchronization regardless of balanced or unbalanced power grid. The double frequency oscillations produces in current due to presence

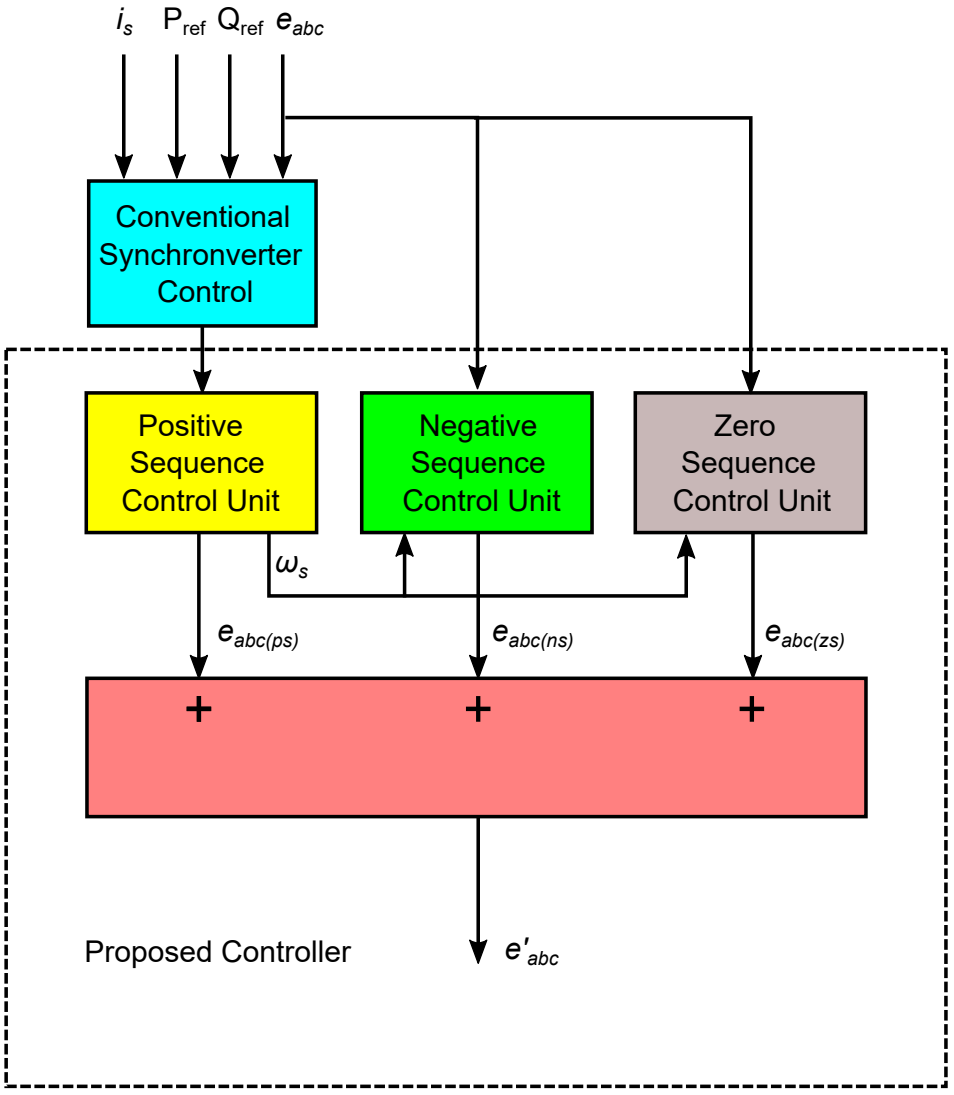

FIGURE 2.10: Block Diagram of Enhanced PLL based Synchronizer [64]

of negative sequences when connected to an unbalanced grid. This scheme has capability to suppress these double frequency oscillations. The block diagram is shown in Figure 2.11.

The limitations of this scheme is mentioned in following points.

- The positive-negative sequence decomposition requires additional processing power.
- Being a conventional virtual current based self synchronizer [34] it cannot provide power to critical local load during synchronization process [46].

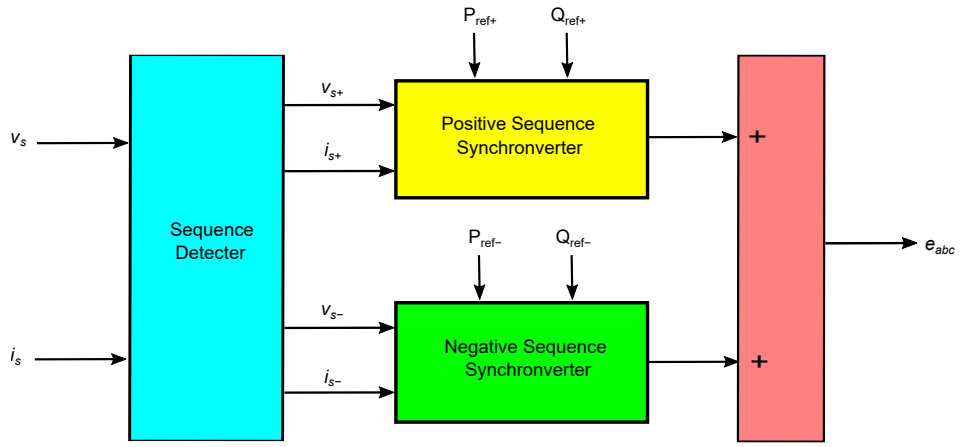

FIGURE 2.11: Block Diagram of Positive-Negative sequence based self-synchronizer [65]

2.3.2.4 Resonant Controller Based Self-synchronizer [40]

In this approach, the standard virtual current based self-synchronized synchronverter is equipped with filter-based current feeding loops. It improves its stability and suppresses the power ripples in presence of unbalanced grid.

Furthermore, the features of the traditional synchronverter in unbalanced power grids are examined, and a better approach to regulate power ripples and current harmonics is suggested, utilizing a resonant controller. The block diagram is shown in Figure 2.12.

The limitations of this scheme are mentioned in following points.

- Due to inclusion of additional control loops and filters the complexity and computational burden is increased.
- Additional filters have also increased the complexity.
- As this scheme is based on conventional virtual current based self synchronizer [34], it cannot provide power to critical local load during synchronization process [46].

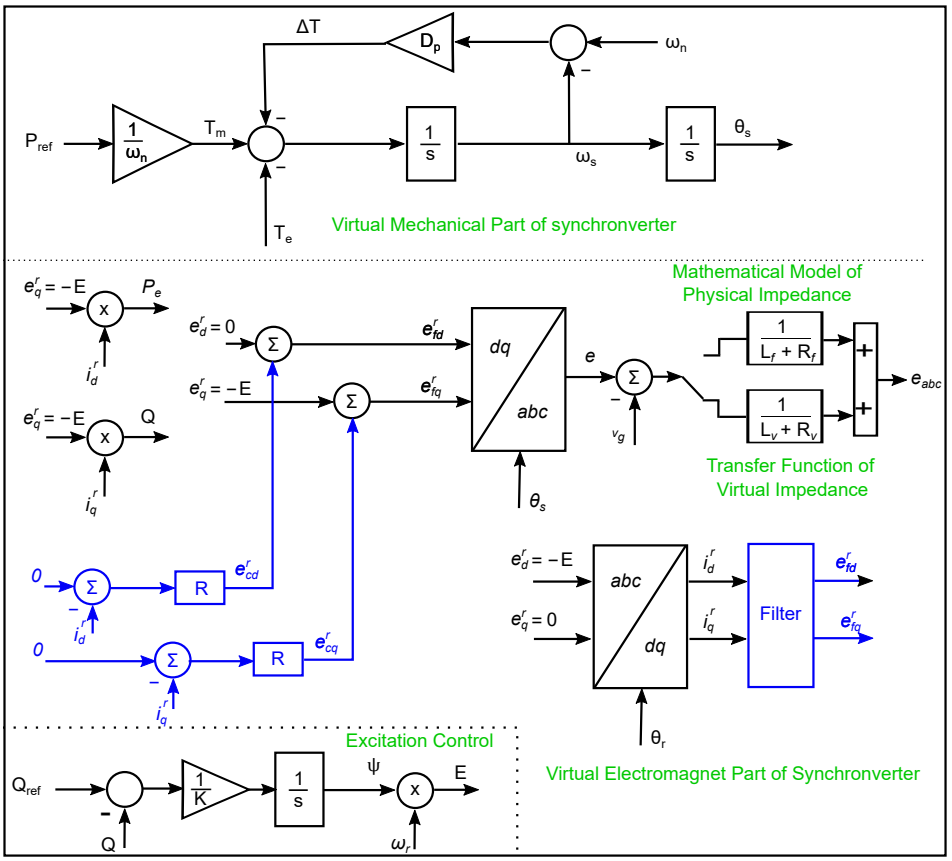

FIGURE 2.12: Block Diagram of Resonant controller based self-synchronizer [40]

2.3.2.5 Lyapunov Energy Function Based Direct Power Controller [66]

The operation of the synchronverters is complicated by second harmonic oscillations in the active and reactive power when the grid voltage are unbalanced.

In this scheme, a direct power control based on Lyapunov energy function has been implemented to control the power fluctuations and eliminate them during grid voltage unbalance.

The implementation of this scheme requires symmetrical components of unbalanced grid. To fulfill this need a popular architecture of the dual second order generalized integrator DSOGI PLL is used. It can extract the positive and negative sequence components of voltages and current. The block diagram is shown in Figure 2.13.

The limitations of this scheme is mentioned in following points.

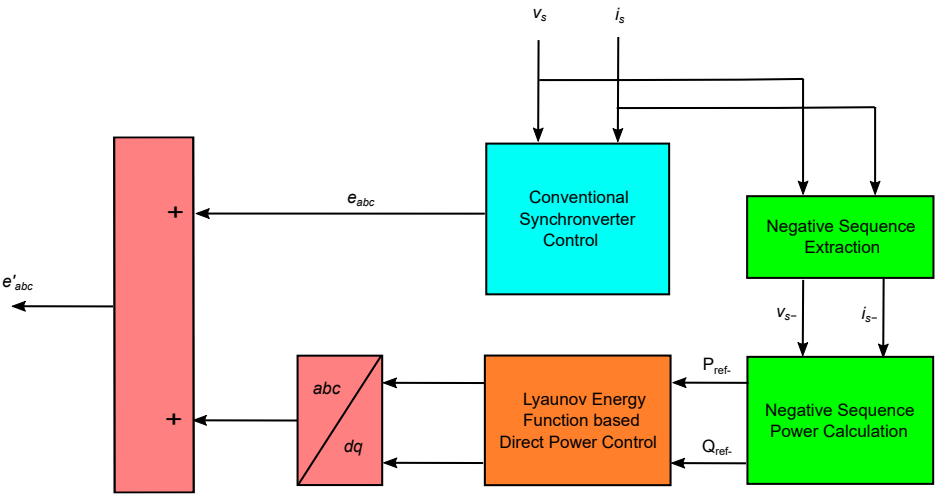

FIGURE 2.13: Block Diagram of DPC based Synchronizer [66]

TABLE 2.3: Comparison of pre-synchronization techniques of synchronverter for an unbalanced grid

Technique	**Reference**	**Hot-Seamless Capability**	**PLL**
Positive sequence based Self-synchronizer	[61]	No	No
Enhanced PLL based Synchronizer	[64]	Yes	EPLL
Positive Negative sequence based Self-synchronizer	[65]	No	No
Resonant controller based self-synchronizer	[40]	No	No
Direct power control based scheme	[66]	Yes	DSOGI PLL

- The addition of extra control loops has increased the complexity.
- The computational load has also increased due to additional loops.
- The use of dual second order generalized integrator DSOGI-PLL can cause uncertainties.

2.4 Applications of Synchronverter

The synchronverter technology has distinguished itself from other inertial emulation topologies presented in the literature for power converters because of its adaptability to a wide range of applications. Static compensators, wind turbines, electric cars, HVDC networks, DC micro-grids and grid-connected distributed energy resources are among the potential applications for the synchronverter technology. Following are the application found in literature.

2.4.1 Integration of Energy Storage Devices

The incorporation of the Synchronverter strategy with a bank of Lithium-ion batteries for connection to the electrical grid were proposed in [67]. In this case, a bidirectional DC/DC converter is used to connect the battery bank to the DC bus and subsequently, the synchronverter performs the power transfer from the DC bus to the AC network. The authors propose to incorporate a load management algorithm to the system control of the synchronverter in order to achieve maximum performance with the contribution to system stability by providing inertial response and meeting fault ride-through requirements.

In the study by [68], they introduced the use of a Static Var Compensator (SVC) with a battery holder to operate in a weak network. The purpose was to provide voltage support and virtual inertia to the system. The SVC controls the active and reactive power injected into the network, while the DC/AC converter is associated with it. A study is done in [69] for integration of Energy Storage System Using Synchronverter-Based converter.

2.4.2 Integration of Solar Panels

The integration of a STATCOM with solar photovoltaic systems (PV) represents another potential application. In a study by [70], a PV system was operated with MPPT control. In this type of system, the synchronverter also plays a role in

controlling the voltage in the DC-link. As a result, the difference between the input voltage of the synchronverter and its reference value goes through a PI block, whose output is then subtracted from the active power reference. In [71] a single stage three phase PV system is proposed for grid integration of solar panels. [72] proposed a single phase solar photovoltaic system for providing machine learning based virtual inertia by synchronverter. In essence, the single-phase synchronverter enables the photovoltaic system to provide ancillary services such as inertial response, frequency, and voltage support in response to variations in the network.

2.4.3 Integration of Wind Turbines

The application of the Synchronverter technology can be extended to back-to-back power converters that are driven by Pulse Width Modulation (PWM) modulation, which is commonly used to connect variable speed wind turbines to the power system. The strategy initially introduced by Zhong [73] involves applying the synchronverter philosophy to both converters in the wind energy conversion system i.e. the AC/DC converter (rectifier) and the DC/AC inverter. In short, the turbine-side converter i.e. rectifier functions as a synchronous motor, with the respective system control unit responsible for regulating the voltage in the DC link and operating under unity power factor. At the same time, the grid-side converter i.e. inverter operates as a synchronous machine with the goal of controlling and maximizing power extraction from the wind referred to as Maximum Power Point Tracking (MPPT) and regulating the reactive power injected into the network [73].

2.4.4 HVDC Systems

High Voltage Direct Current (HVDC) transmission systems, operating with Voltage Source Converter (VSC) converters and vector control, are considered one of the most suitable technologies for integrating renewable energies into the power grid [74, 75]. However, the HVDC topology may become unstable when connecting

weak networks that demand high power and do not provide an inertia value for the system. [76] proposed the application of Synchronverter (synchronverter) to the rectifier control system, where strategies based on voltage and power were developed. By applying these strategies to an HVDC system, the network perceives the terminal that sends power as a virtual synchronous motor powered by the AC network and the receiving terminal as a virtual synchronous machine who's DC-link represents the virtual mechanical torque (Aouini et al., 2015). An HVDC system operating with synchronverter is called Synchronverter HVDC (SHVDC) [77]. An SHVDC system can provide inertial behavior to the grid, but a synchronous machine with the same nominal value as the VSC would result in low performance. This would lead to greater fluctuations in waveforms and increased variations in the face of disturbances on the network. [78] have developed an analytical method for adjusting the parameters used in SHVDC. This method is based on sensitivity analysis of the system poles in relation to control parameters and the location of poles. The results demonstrate that in this case, the synchronverter can provide even more satisfactory performance than vector control.

2.4.5 Static VAR Compensator and STATCOM

The capability of using a synchronverter as a static synchronous condenser (STATCOM) with voltage imbalance compensation functionality was discussed by [79]. In [80] suggested to operate the STATCOM as a virtual synchronous condenser, as current controllers for STATCOM operation generally do not inherently consider the model of synchronous machines. The authors suggested adding an extra control loop droop ('D-mode') to enable the parallel operation of STATCOMs for sharing reactive power based on voltage variation.

2.4.6 Recharging Electric Vehicles

Electric Vehicles (EVs) are expected to play a significant role in modern electrical networks in the near future [81]. From the perspective of the network, EVs can be

seen as small battery banks that are intermittently connected to the grid. In order to prevent the growing number of EVs from necessitating an expansion of the grid to accommodate peak demand, loading/unloading systems known as Vehicle-to-Grid (V2G) have been developed [82, 83]. This technology allows EVs to provide support services to the grid and using the charge stored in their batteries, help mitigate peak demand by adjusting the power delivered or received based on the state of charge (SoC) of the connected EV batteries.

Additionally, with the application of Supervisory Control and Data Acquisition (SCADA) to V2G, EVs can contribute to the grid's equivalent inertia, further assisting with ancillary services [82]. Similarly, the concept of variable inertia can be extended to V2G stations [83] with the implementation of an adaptive controller that determines the inertia value based on the battery SoC.

2.4.7 DC Microgrids

DC microgrids have several advantages like no reactive power present and no need for frequency synchronization circuits. Additionally, conductors do not confront a skin effect, there is a smaller number of cables compared to three-phase systems and reduced electromagnetic emission [84].

Despite these advantages, voltage is the only control parameter in microgrids, making power sharing between different converters in the system more difficult to achieve with balanced distribution. This difficulty may lead to overload in some system converters while neglecting others. To address this issue, the proposed model by [85, 86] allows the use of the supervisory voltage (synchronverter) to control converters.

The synchronverter helps impose a low ripple amplitude and frequency as a function of the energy state of the network, facilitating communication between various circuit sources and enabling power sharing between different sources with locally measured variables.

2.5 Gap Analysis

The synchronverter has received particular attention among all virtual synchronous machines (VSMs) because of its comparable dynamics with a synchronous machine. Thus, synchronverter design and its performance have been the subject of several challenges and concerns raised by scholars over the last ten years. In Section 2.1, several adjustments to enhance its functionality have been addressed, along with pre-synchronization methods to accomplish the initial synchronization with balanced or unbalanced grid.

There is an issue regarding the pre-synchronization of synchronverter with an unbalanced grid which are unsolved. The research gap in this field is stated as under.

- In critical load applications e.g. hospitals or military units, the pre-synchronizer of synchronverter must continue its output power during pre-synchronization process. To achieve this, a hot-seamless pre-synchronization scheme is required.
- Researchers have proposed hot-seamless schemes for synchronverter which work only with a balanced grid but no PLL-Less scheme is proposed in literature which can achieve a hot-seamless pre-synchronization of synchronverter with an unbalanced grid.

2.6 Problem Statement and Solution

An enhanced pre-synchronizer is needed for pre-synchronization of synchronverter with an unbalanced grid. It should be able to function without the use of a Phase locked loop (PLL). Moreover, it can achieve the pre-synchronization of synchronverter with an unbalanced grid while ensuring uninterrupted power to the local critical load. The transient currents at the time of grid connection should be minimum.

Solutions Proposed:

For enhancement of the pre-synchronization of synchronverter with an unbalanced grid, an improvement in existing Fourier analysis based PLL-less self-synchronizer [46] is proposed here that

(a) ensures hot-seamless transfer of synchronverter from standalone to grid-connected mode.

(b) prevents the tripping of synchronverter by significantly reducing the voltage difference and inrush synchronverter currents during pre-synchronization with a three phase grid having unbalance in its voltage or phase angle.

(c) can achieve pre-synchronization of synchronverter with the grid if a sag occurs during pre-synchronization process.

2.7 Research Methodology

Firstly, a method of decomposing the unbalanced grid voltages into its symmetrical components in frequency and time domain is derived using Fortescue Transform. Then the Lyon transformation is implemented to extract the instantaneous positive sequence vectors of unbalanced grid.

Secondly, a positive sequence extraction block (based on Lyon transformation) is embedded in existing PLL-Less Fourier Analysis based self-synchronizer to make it capable of achieving a successful pre-synchronization of synchronverter with an unbalanced grid.

At last, the enhanced pre-synchronizer is tested in four different scenarios and the results are compared for its validation. All research work is based on simulations carried out in MATLAB R2023a/Simulink using the SimPowerSystem tool.

2.8 Applications of Enhanced Pre-synchronizer

The applications for synchronverter include Renewable energy resources (RERs) integration in power grid, modular multilevel converters, HVDC transmission Network, Synchronous rectifier, static Compensators, Electric Vehicle Charging stations, and Energy Storage integration. Any application where a synchronverter with a local linked load has to be synced with an unbalanced grid can use the proposed pre-synchronizer. Below is a list of a few of the applications:

- The residential and commercial applications where roof-top PV plants required to be operated in both standalone and grid-connected mode.
- Connection of Microgrids having local critical loads in remote areas where grid is weak and the voltages of grid do not remain balanced.
- Electric Vehicles (EVs) charging and discharging systems for Vehicle to grid (V2G) support.
- The integration of distributed energy generation based power plant supplying critical centers like data centers, hospitals, military units etc into the power grid

Chapter 3

Design of Enhanced Pre-synchronizer

The synchronverter is capable of staying synchronized with the grid without the need for a dedicated synchronization unit. It can seamlessly do transition from grid-connected to standalone mode without requiring any adjustments to the controller. However, it does require a synchronizer to monitor the grid phase and frequency as a reference before connecting to the grid [46].

The grid voltages do not remain balanced in all distribution networks specially in the weak grid which usually presents steady state unbalanced voltages due to single phase loads. In addition the Pakistan Grid code 2023 (CC 6.2.1 para (e)) put a restriction on solar and wind power plants to remain synchronized with the transmission system during a negative phase sequence load unbalance of 5% of positive sequence component.

Several PLL-Less techniques have been developed by researchers for synchronization of the synchronverter before grid connection. Mostly, these schemes are designed by considering an ideally balanced grid, relatively a little work has been done for initial synchronization with an unbalanced or weak grid. Moreover a synchronization scheme must posses a hot-seamless capability in such applications

where critical local loads are present. Hot-seamless capability defines that the supply to critical loads like hospital or military installations must not be interrupted during pre-synchronization process.

A few PLL-Less schemes has been reported in literature [46],[38] that can achieve hot-seamless synchronization. But these schemes works well only with a balanced grid. To the best knowledge of author, no PLL-Less scheme is designed that can achieve hot-seamless pre-synchronization with an unbalanced grid.

In this chapter, the performance of existing FA-based PLL-Less self-synchronizer [46] is analyzed for pre-synchronization of synchronverter with an unbalanced grid, a method extracting instantaneous symmetrical components of unbalanced grid is derived using Fortescue and Lyon transformation [61], a Fourier Analysis based PLL-Less self-synchronizer is modified to overcome its limitations regarding pre-synchronization of synchronverter with an unbalanced grid.

3.1 Fourier Analysis Based PLL-Less Self Synchronizer

The self synchronizer proposed in [46] is motivated by fourier Series. Figure 3.1 shows the block diagram of proposed synchronizer. In this scheme the grid phase angle θ_g is measured by doing the fourier analysis of grid voltage v_{ga}.

During synchronization process, depending upon the magnitude and sign of the phase difference between v_{sa} and v_{ga}, the synchronverter angular frequency ω_{syn} and voltage v_s are adjusted by respective PI controllers. The process continues until the rms difference between v_{sa} and v_{ga} reaches the threshold value i.e. 12V in this case and then PCC breaker is closed to share the power with grid. Since the local load has to be supplied during the synchronization process, the maximum value of ω_{syn} can be varied by $\pm\pi\ rad/s$.

The conventional synchronverter with existing FA-based synchronizer tracks only phase a of the grid therefore during synchronization with an unbalanced grid it

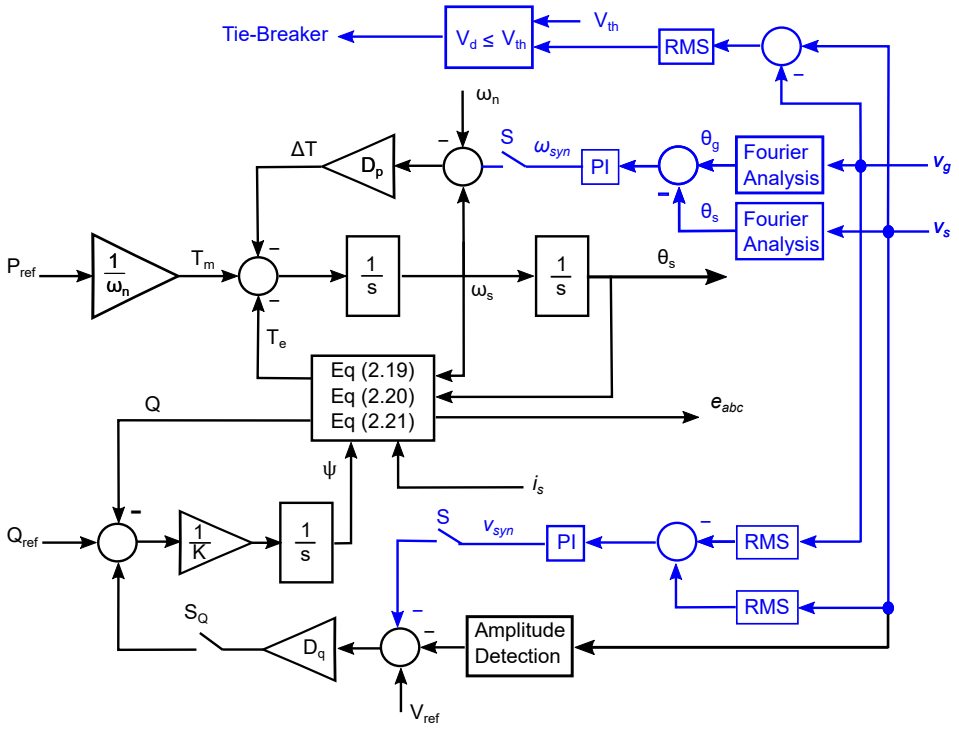

FIGURE 3.1: Block diagram of FA-based PLL-Less self-synchronizer [46]

will close the PCC breaker regardless the threshold value ($12V$) between other two phases has not been achieved.

Figure 3.2 and 3.3 shows the RMS values of instantaneous difference between synchronverter and grid voltages during synchronization process with a balanced and unbalanced grid respectively.

It is clear from figure 3.2 that when the PCC breaker is closed the difference between all phases is below the threshold value of 12V in case of a balanced grid but figure 3.3 shows that when the grid is unbalanced the difference of phase b and c is 46V and 47V respectively which is above the threshold value.

The large difference of phase b and c in case of unbalanced grid can cause high transients in inverter current and can result in the shutdown of inverter or even damage its devices or PCC breaker. In context of above limitation a modification is required in existing FA-based scheme to make it suitable for achieving a seamless synchronization with an unbalanced grid.

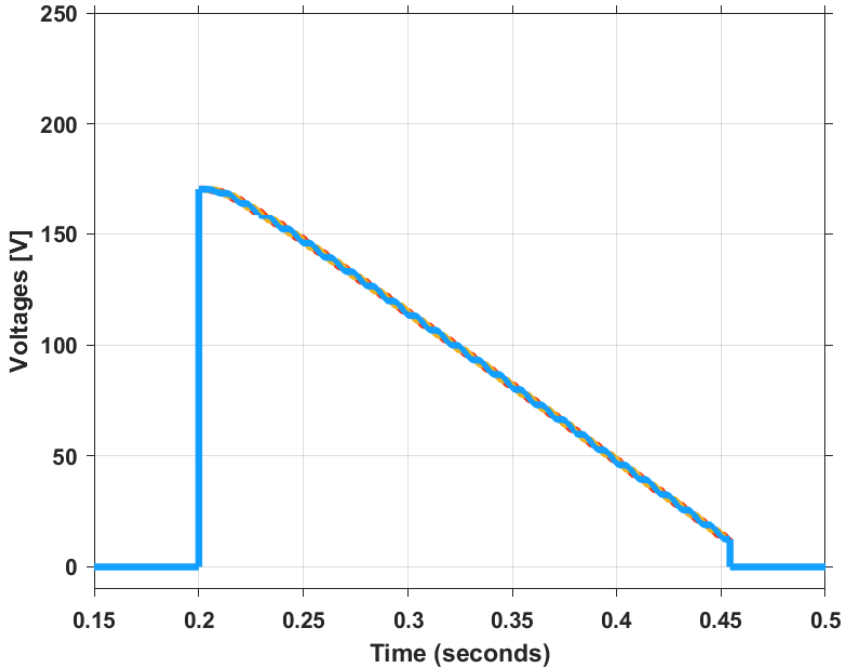

FIGURE 3.2: Pre-synchronization of synchronverter with a balanced grid using FA-based PLL-Less self-synchronizer

The control of synchronverter generates positive sequences at its output and its control is designed to operate only with a balanced grid. The synchronverter can be synchronized with an unbalanced grid using FA-based PLL-Less self-synchronizer if the instantaneous positive sequences of grid are used.

In the following section a method of extracting instantaneous positive sequences of grid is derived and implemented using Fortescue and Lyon transformation [61].

3.2 Space Vector based Symmetrical Decomposition

Three voltages along with three currents work together in three phase electric systems to deliver the loads both active and reactive power. According to conventional theory, a set of three phase balanced signals have the same magnitude

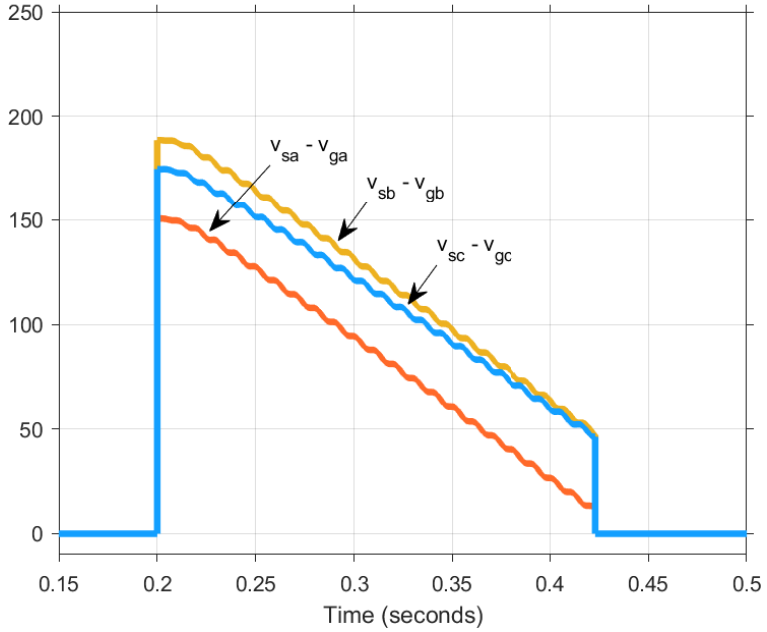

FIGURE 3.3: Pre-synchronization of synchronverter with an unbalanced grid using FA-based PLL-Less self-synchronizer

and 120° electrical rotational separation. This assumption holds true for transmission systems, but due to single-phase and two-phase loads, as well as power grid asymmetry, not all distribution networks hold for such a balance scenario.

More specifically, power converters require space vector transformation to address these unbalances. The upcoming section present the symmetrical component decomposition of three phase signals in the time and frequency domains.

3.2.1 Symmetrical Components in Frequency Domain

Power converters connected to the grid are extremely vulnerable to voltage fluctuations at the common coupling point (PCC). It is crucial to accurately detect the unbalanced voltage vector when considering sensitivities. To achieve this sort of detection, the method of symmetrical decomposition was first introduced by Fortescue [62].

Three unbalanced voltage or current signals can be divided into three balanced vectors using this method. Positive, negative and zero sequences are the common

titles for those vectors. The rotation of the positive sequence is counterclockwise, maintaining the abc rotational order. In the meantime, the rotational order of acb is preserved by the negative sequence, which creates a clockwise rotation. In both scenarios, there are three vectors, each separated by 120 deg or $\frac{2\pi}{3}$ radians. Three vectors with the same magnitude are present. Both cases have three vectors separated by 120 deg or $\frac{2\pi}{3}$ radians. The zero-sequence signal consists of three vectors that have the same magnitude and angle, or zero degrees. The following transformation needs to be taken into account in order to change a natural frame into a $(+ - 0)$ frame in the frequency domain:

$$V_{+-0(a)} = [T_{+-0}]V_{abc} \tag{3.1}$$

The subsequent voltage vectors as well as the Fortescue transformation matrix have been obtained after each term is expanded:

$$V_{abc} = \begin{bmatrix} V_a\angle\theta_a \\ V_b\angle\theta_b \\ V_c\angle\theta_c \end{bmatrix}, \quad V_{+-0} = \begin{bmatrix} V_a^+\angle\theta_a^+ \\ V_a^-\angle\theta_a^- \\ V_a^0\angle\theta_a^0 \end{bmatrix} \tag{3.2}$$

$$[T_{+-0}] = \frac{1}{3}\begin{bmatrix} 1 & \alpha & \alpha^2 \\ 1 & \alpha^2 & \alpha \\ 1 & 1 & 1 \end{bmatrix}$$

where $\alpha = e^{j\frac{2\pi}{3}} = 1\angle 120\,\text{deg}$ is the Fortescue operator that maintains the vectors 120 deg apart. The sequence components for phase a in the frequency domain can be found using Eq. 3.1. if needed, phases b and c can also be calculated through Eq. 3.3.

$$\begin{aligned} V^+a\angle\theta_b^+ &= \alpha^2 V^+a\angle\theta_a^+, \\ V^-b\angle\theta_b^- &= \alpha V^-a\angle\theta_a^-, \\ V^+c\angle\theta_c^+ &= \alpha V^+a\angle\theta_a^+, \\ V^-c\angle\theta_c^- &= \alpha^2 V^-a\angle\theta_a^- \end{aligned} \tag{3.3}$$

Regardless of how the voltage or current vectors are expressed in the symmetrical components for the phase a.The conversion to the natural frame can be obtained using following equation.

$$V_{abc} = [T_{+-0}]^{-1} V_{+-0(a)} \tag{3.4}$$

and $[T_{+-0}]^{-1}$ is expressed in Eq. 3.5:

$$[T_{+-0}]^{-1} = \begin{bmatrix} 1 & 1 & 1 \\ \alpha^2 & \alpha & 1 \\ \alpha & \alpha^2 & 1 \end{bmatrix} \tag{3.5}$$

For the frequency domain vectors, the aforementioned formulation is accurate. An adequation has to be implemented when time-domain signal processing of current and voltage vectors is required.

3.2.2 Symmetrical Components in Time Domain

In time domain the symmetrical component decomposition was proposed and developed by Lyon [63]. If Eq. 3.2 by Fortescue is applied to sinusoidal unbalanced waveforms shown in Eq. 3.7, it is possible to obtain the instantaneous vectors as found in Eqs. 3.8 and 3.9.

$$V_{abc} = \begin{bmatrix} v_a \\ v_b \\ v_c \end{bmatrix} = v^+_{abc} + v^-_{abc} + v^0_{abc} \tag{3.6}$$

$$= V^+ \begin{bmatrix} \cos(wt) \\ \cos(wt - \frac{2\pi}{3}) \\ \cos(\omega t + \frac{2\pi}{3}) \end{bmatrix} + V^- \begin{bmatrix} \cos(wt) \\ \cos(wt + \frac{2\pi}{3}) \\ \cos(\omega t - \frac{2\pi}{3}) \end{bmatrix} + V^0 \begin{bmatrix} \cos(wt) \\ \cos(wt) \\ \cos(wt) \end{bmatrix} \tag{3.7}$$

$$v_{+-0(a)} = [T_{+-0}] v_{abc} \tag{3.8}$$

$$v_{+-0(a)} = \begin{bmatrix} \vec{v_+} \\ \vec{v_-} \\ \vec{v_0} \end{bmatrix} = \begin{bmatrix} +\frac{1}{2}V^+e^{jwt} + \frac{1}{2}V^-e^{-jwt} \\ +\frac{1}{2}V^+e^{jwt} + \frac{1}{2}V^-e^{-jwt} \\ V^0\cos(wt) \end{bmatrix} \tag{3.9}$$

The Lyon transformation can be stated in Eq. 3.10 through following normalized matrix, where $[T'_{+-0}] = [T'_{+-0}]^T$.

$$[T'_{+-0}]^T = \sqrt{3}[T'_{+-0}] = \frac{1}{\sqrt{3}} \begin{bmatrix} 1 & \alpha & \alpha^2 \\ 1 & \alpha^2 & \alpha \\ 1 & 1 & 1 \end{bmatrix} \tag{3.10}$$

It can be confirmed from Eq. 3.9 that the resulting vector consists of a real term $\vec{v_0}$ and two complex terms $\vec{v_+}$ and $\vec{v_-}$. It is possible to derive the complex terms $\vec{v_+}$ and $\vec{v_-}$ into instantaneous space vectors having opposing rotations and a similar amplitude.

The positive and negative sequence voltage vectors, v^+_{abc} and v^-_{abc}, are not the same as these terms; on the other hand, the $\vec{v_0}$ is directly connected to the zero sequence components of the original three phase voltage vector. To extract the negative and positive sequence vectors v^-_{abc} and v^+_{abc} from an unbalanced input vector v_{abc}, the Fortescue operator α needs to be transformed from frequency domain to time domain. Consequently, a time-shifting operator must be applied, which is commonly accomplished by $\frac{2}{3T}$, where $'T'$ is signal period.

The shifting operator is equivalent to 120 deg as the entire period is equal to 360 deg. Another way to express the Fortescue operator is as follows: $\alpha = -\frac{1}{2} + j\frac{\sqrt{3}}{2}$. A filter can be used to produce 90deg phase-shifting associated with the imaginary operator $'j'$,. This delay can be used to implement the time-shifting operator [63]. A simplified implementation of the time-shifting operator α is shown in Figure 3.4(a), where the damping factor $\zeta = 1$ and a second-order low-pass filter (LPF) is adjusted at the input frequency ω_{in}. As shown in Figure 3.4(b) the α^2 operator can be computed by simply multiplying the output signal of Low pass filter (LPF) by -1.

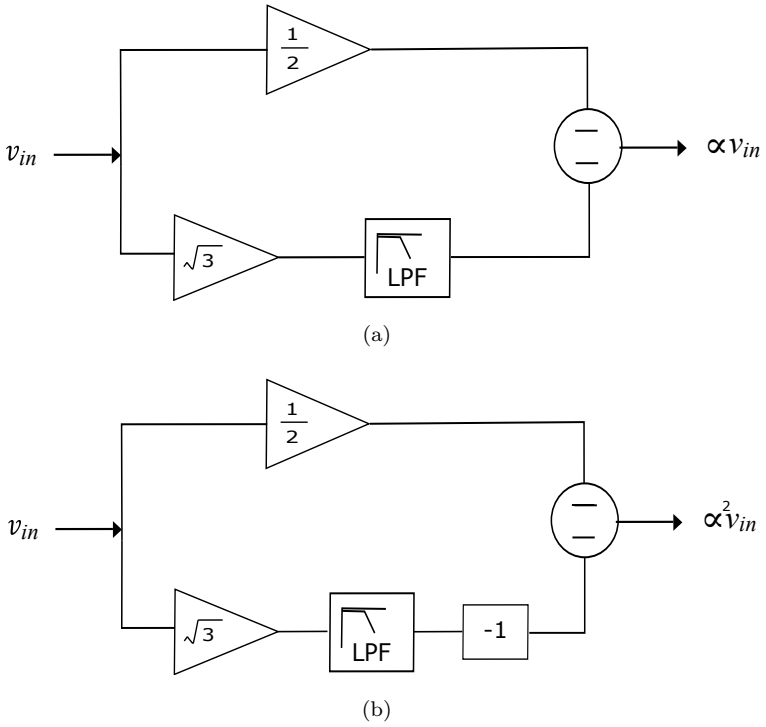

FIGURE 3.4: Block Diagram of Time-shifting operator implementation (a) α (b) α^2 [87].

The LPF can be calculated as in Eq. 3.11.

$$LPF_(s) = \frac{\omega_{in}^2}{(s + \omega_{in}^2)} \tag{3.11}$$

3.3 Enhanced FA-based PLL-Less Self Synchronizer

In this section the existing FA-based self-synchronizer is enhanced to overcome its limitations described in section 3.1. In this proposed scheme, a Positive sequence extractor (PSE) block based on the method formulated in section 3.2 has been added in existing FA-based self-synchronizer which decomposes the unbalanced grid voltages into its instantaneous symmetrical components without using a PLL. Figure 3.5 shows the block diagram of proposed scheme.

In Positive sequence extractor (PSE) block, each vector of grid voltage is split into a, b, and c phases and introduced to the time shifting circuits presented in Figure

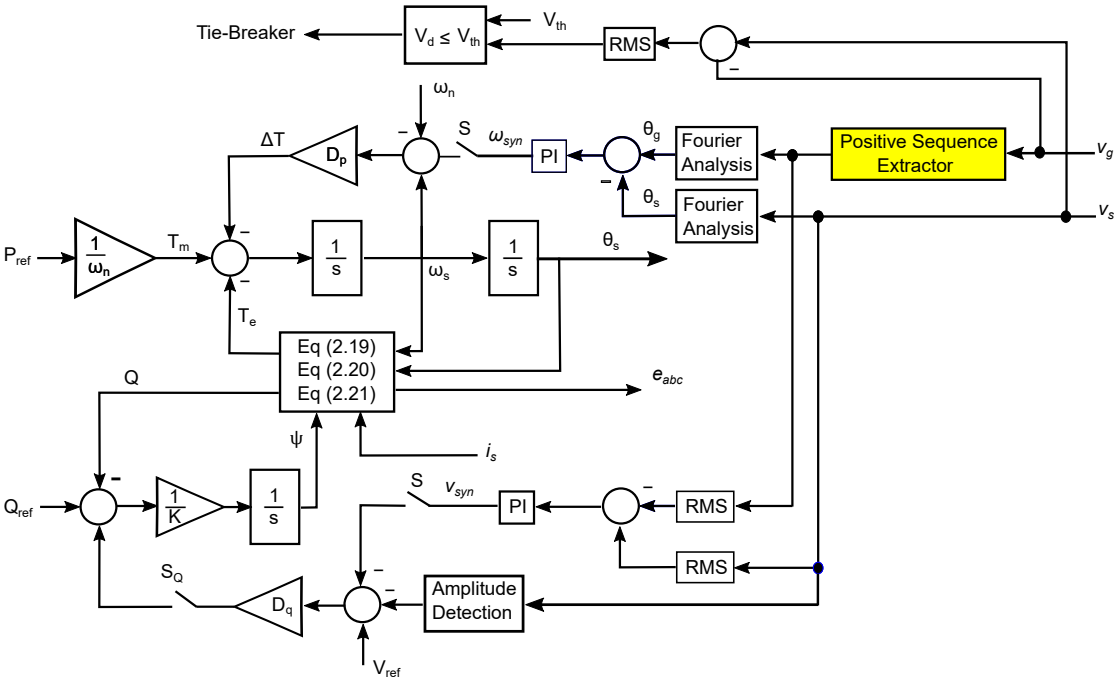

FIGURE 3.5: Block Diagram of Proposed enhanced FA-based PLL-Less self synchronizer.

3.4. As a result, each single phase has three resulting signals: the original (v_{ga}, v_{gb}, v_{gc}), the one shifted by the Lyon operator (αv_{ga}, αv_{gb}, αv_{gc}), and the one shifted by the square Lyon operator($\alpha^2 v_{ga}$, $\alpha^2 v_{gb}$, $\alpha^2 v_{gc}$).

Then, the per phase instantaneous positive sequences are calculated using the resulting signals, as per Eq. 3.12.

$$v^+_{abc} = \begin{bmatrix} v^+_a \\ v^+_b \\ v^+_c \end{bmatrix} = \frac{1}{3} \begin{bmatrix} v_a & \alpha v_b & \alpha^2 v_c \\ \alpha^2 v_a & v_b & \alpha v_c \\ \alpha v_a & \alpha^2 v_b & v_c \end{bmatrix} \tag{3.12}$$

Chapter 4

System Design and Simulation Results

In this chapter the basic parameters calculation for the design of synchronverter using enhanced pre-synchronizer is presented. Moreover, the designed synchronverter is simulated in different grid scenarios using existing and enhanced pre-synchronizer. The performance of both schemes is compared in results.

The block diagram of complete system with enhanced pre-synchronizer is shown in figure 4.1

4.1 Design of Complete System using Enhanced Pre-synchronizer

Figure 4.2 shows the complete schematic diagram of the synchronverter with proposed enhanced pre-synchronizer. In power part, the DC source is considered ideal for simplicity. The IGBT switches with anti-parallel diodes are used in three phase PWM Inverter that performs the DC-AC conversion. Instantaneous phase values of grid voltage (v_g), synchronverter output voltage (v_s) and output current (i_s) is measured by two measurement blocks MT2 and MT1 respectively.

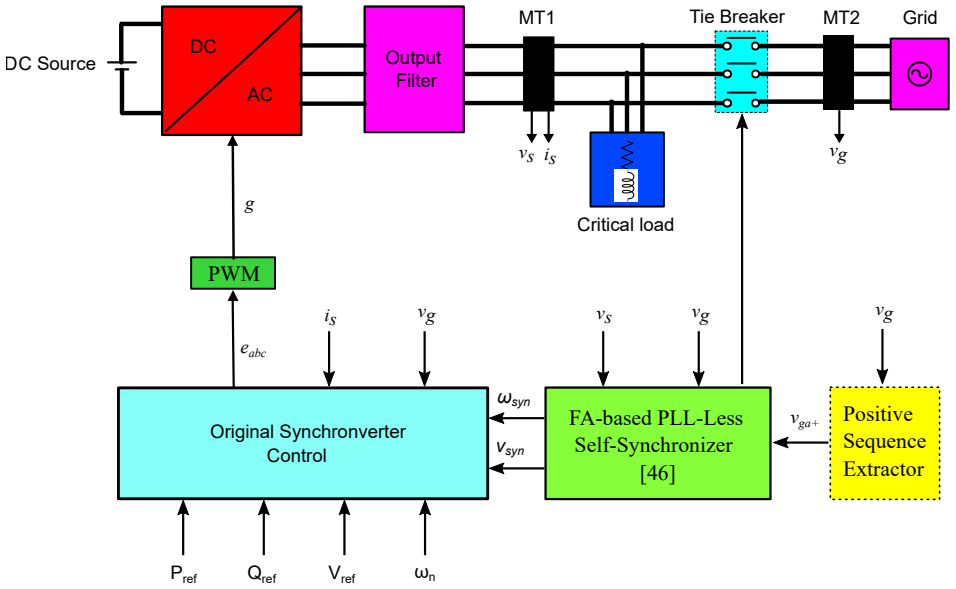

FIGURE 4.1: Block Diagram of Complete system with enhanced FA-based self-synchronizer.

An LCL filter is used at the output of inverter stage for PWM filtering because this filter topology offers lower voltage drop and better damping characteristics than LC filter [88]. The detailed filter designing is presented in [88, 89].The controller has two parts, the original synchronverter control and enhanced pre-synchronizer.

The conventional synchronverter controller part incorporates the original synchronverter model proposed in [34]. In this controller the synchronous generator model block implements the mathematical model of a synchronous generator derived in 2. This model consists of the mathematical computation of electrical torque, induced electromotive force and reactive power given in Eq. 4.1 to 4.3.

$$T_e = \psi \, s \, \langle i_s, \widetilde{\sin}\theta_s \rangle \tag{4.1}$$

$$e_{abc} = \omega_s \, \psi \, \tilde{\sin} \, \theta_s \tag{4.2}$$

$$Q = -\omega_s \, \psi \, s \, \langle i_s, \widetilde{\cos}\theta_s \rangle \tag{4.3}$$

Where ψ_s is the magnetic flux, ω_s is the angular speed and θ_s is the rotor angle of the synchronverter. In Figure 4.2 the upper half part of the controller is the

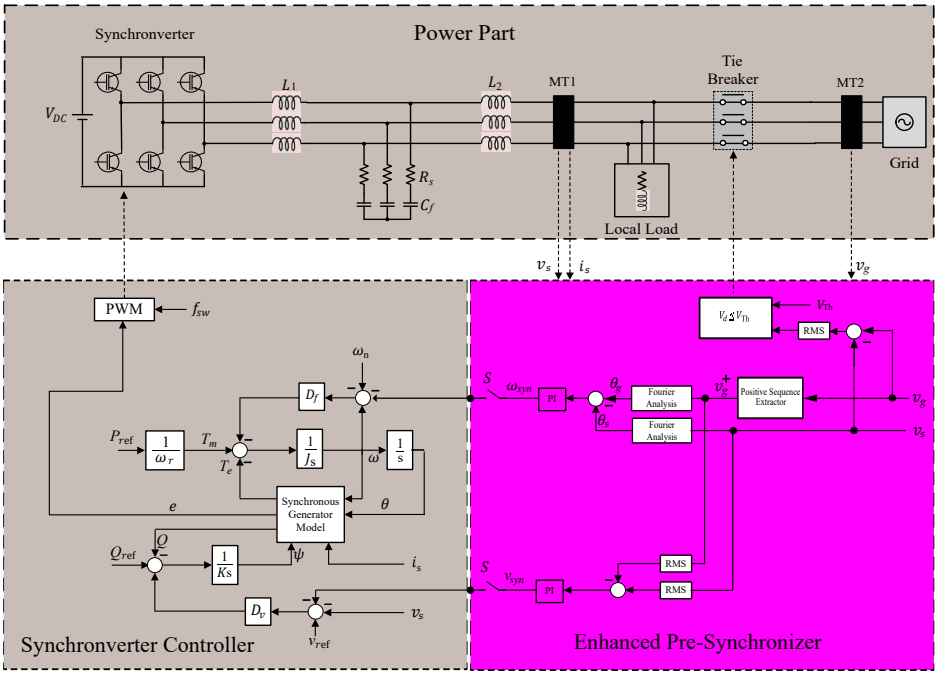

FIGURE 4.2: Complete system with enhanced pre-synchronizer

frequency control loop. It is based on swing equation of synchronous generator as given in Eq. 4.4.

$$J\,\dot{\omega} = T_m - T_e - D_f(\omega_s - \omega_n) \tag{4.4}$$

Where D_f is the damping coefficient and J is the virtual inertia of synchronous generator. The damping coefficient D_f maintains the steady state stability while the virtual inertia J (like the real inertia of synchronous generator) provide support to the grid during disturbances [90]. D_f and J both are chosen by Eqs. 4.5 and 4.6. The complete design of these parameters is elaborated in [34][91].

$$D_f = -\frac{\Delta P_s}{\omega_s\,\Delta w_s} \tag{4.5}$$

$$J = D_f\,\tau_\rho \tag{4.6}$$

Where τ_ρ is the time constant for the frequency control loop. The lower half part of the synchronverter controller is a voltage control loop. D_v is the voltage droop

coefficient and K is the integrator gain. Eqs. 4.7 and 4.8 are used for designing both parameters. The detailed design is found in [91].

$$D_v = -\frac{\Delta Q}{\Delta v_s} \tag{4.7}$$

$$K = \omega_s \, D_v \, \tau_q \tag{4.8}$$

Where τ_q is the time constant of the voltage control loop. All other parameters of synchronverter are mentioned in 4.1 .

In enhanced pre-synchronizer, the three phase grid voltages v_g are fed to the positive sequence extractor block that transforms v_g into its instantaneous positive sequence vectors. The fourier analysis blocks obtain the phase angle θ_g^+ and θ_s from extracted positive sequence voltages of grid and synchronverter terminal voltage respectively.

Depending upon $\theta_s - \theta_g^+$, the PI controller in upper part generates the frequency correction signal ω_{sync} for phase synchronization. Similarly, PI controller in lower part generates the voltage correction signal v_{sync} for amplitude synchronization. The switch 'S' starts the synchronization process and disconnects the pre-synchronizer when Tie-Breaker is closed.

4.2 Results and Discussion

The circuit was made in Matlab/Simulink version 2023a. The three phase synchronverter having a local load at its output and connected to the power grid through a three pole controlled circuit breaker . A "Universal Bridge" mask and a "2-Level PWM Generator" mask together were used to generate the SPWM. The synchronverter control block provided the reference voltage e_{abc} for PWM Generator mask.

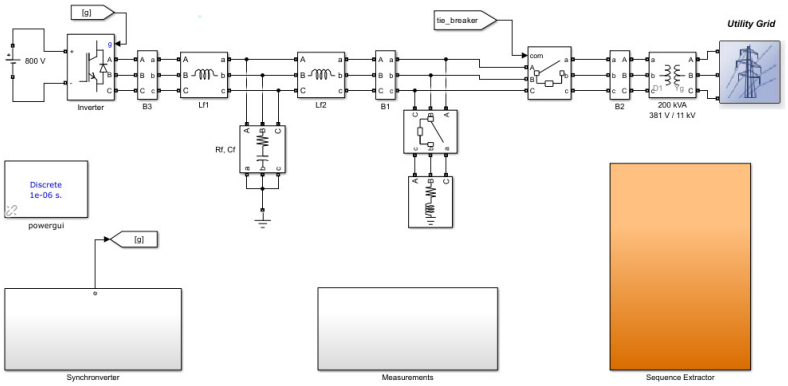

FIGURE 4.3: Block Diagram of System.

The total time of simulation was adjusted to 2 seconds for simulating the standalone, pre-synchronization and grid-connected modes of operation of the synchronverter. The system is presented in Figure 4.3.

The model parameters for system simulation are given in Table 4.1. The synchronization of synchronverter is carried out in four different scenarios of grid, using both existing and enhanced pre-synchronizer. The first scenario tests the performance with a balanced grid, the second scenario considers an unbalanced grid voltage. In third scenario, the grid phase angle are unbalanced and lastly, an unbalanced sag is generated in grid voltage during pre-synchronization process. A comparison of both schemes is performed in the results of all scenarios. The dashed curves indicates the results of the existing scheme, while the solid lines illustrate the results of the proposed scheme. The results of all scenarios are presented in following subsections.

4.2.1 Pre-synchronization while the Grid Voltage are Balanced

A "Three-phase programmable generator" mask in MATLAB/Simulink with a phase-phase voltage amplitude of $381\sqrt{2}/\sqrt{3}$ was used to simulate a balanced grid. In Standalone mode the real and reactive power of local load was used as a reference power for the inverter that changes to 230 KW and 100 Kvar respectively when the pre-synchronization is completed. Figures 4.4 to 4.10 shows the results

TABLE 4.1: Parameters for simulations.

Symbol	Parameter	Value
V_{DC}	DC Bus Voltages	800 V
V_n	Nominal Phase Voltage	220 V-rms
S_n	Nominal Power	250 kVA
f_n	Nominal Frequency	50 Hz
J	Virtual Inertia	1.0132
D_v	Voltage Droop Coefficient	16070
D_f	Damping Coefficient	506.6
K	Integrator Gain	100970
τ_p	Frequency Loop Time Constant	0.002 s
τ_q	Voltage Loop Time Constant	0.02 s
L_1	Filter Inductor	0.3111 mH
L_2	Filter Inductor	0.0587 mH
R_f	Series Resistor	0.0737 Ohm
C_f	Filter Capacitor	91 uF
f_{sw}	Switching frequency	8 kHz
P_v	Proportional Gain	0.1
I_v	Integral Gain	2.3
P_ω	Proportional Gain	0.4
I_ω	Integral Gain	3.4
V_{Th}	Threshold Voltage	12 V
	Local Load	200 + j20 kVA

of this scenario. The simulation was started at 0sec in standalone mode. It

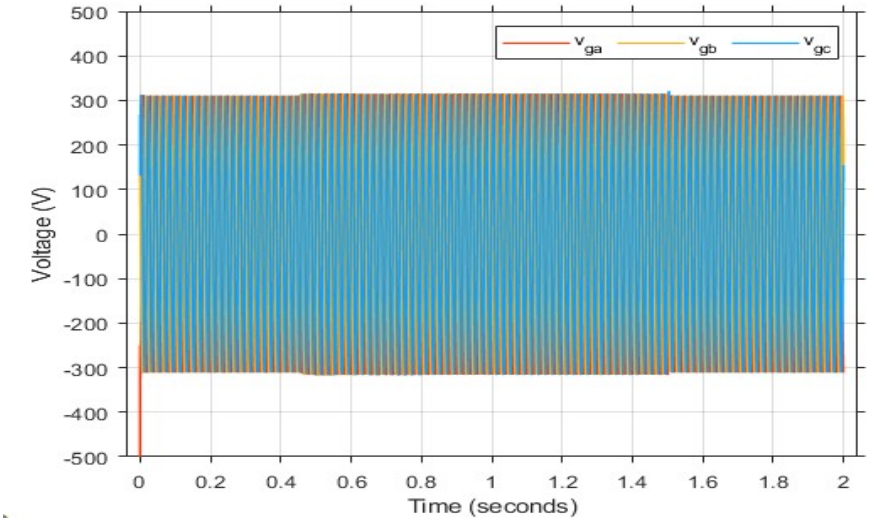

FIGURE 4.4: Grid voltages

can be observed in Figure 4.9 and 4.8 that after the transient period passed the synchronverter maintained its frequency and voltage (at nominal values) for the

local load. The synchronization process was started at 0.2s and got synchronized within 276 msec correctly at 0.46 sec.

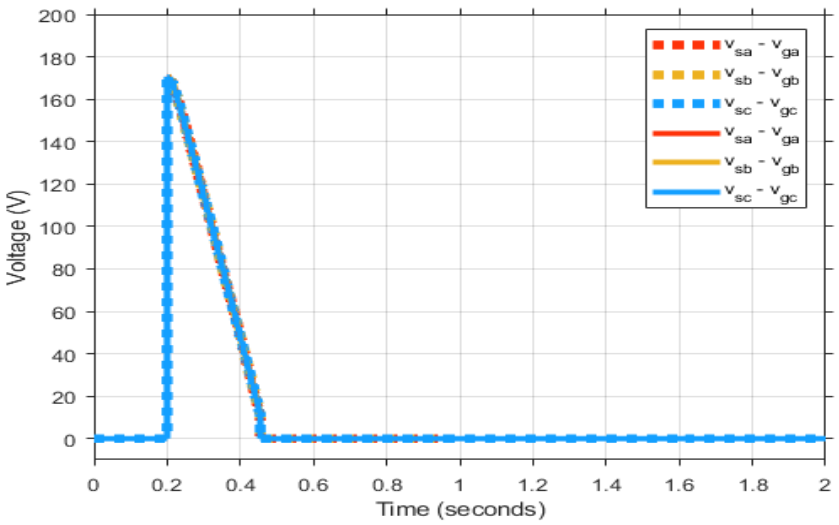

FIGURE 4.5: RMS value of instantaneous difference between synchronverter voltage and grid voltages

The synchronization process is shown in Figure 4.5 to 4.7. It can be observed that the initial difference between the voltage of the Synchronverter and grid was 165V which started decreasing when the pre-synchronizer causes to adjust the Synchronverter frequency and voltage within acceptable limits.

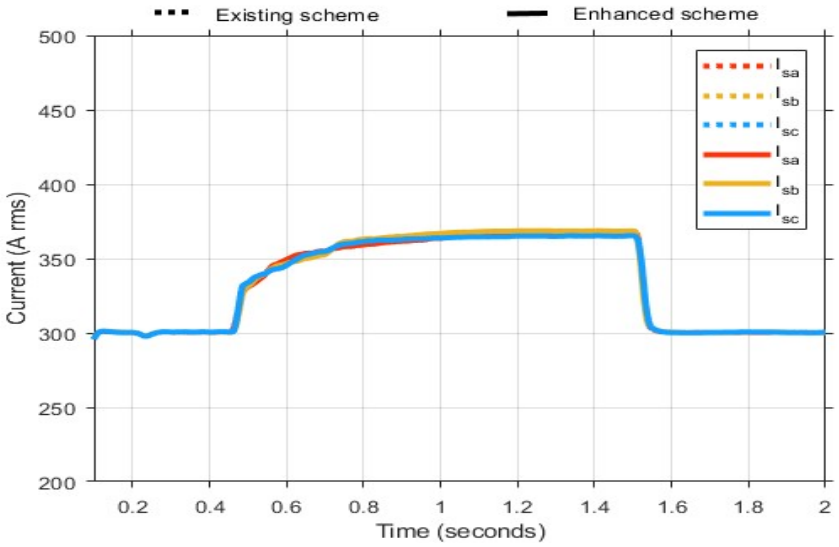

FIGURE 4.6: synchronverter rms currents

The Load current in Figure 4.9 proves that the Synchronverter did not stopped the power supply to Local load during synchronization. On completion of the

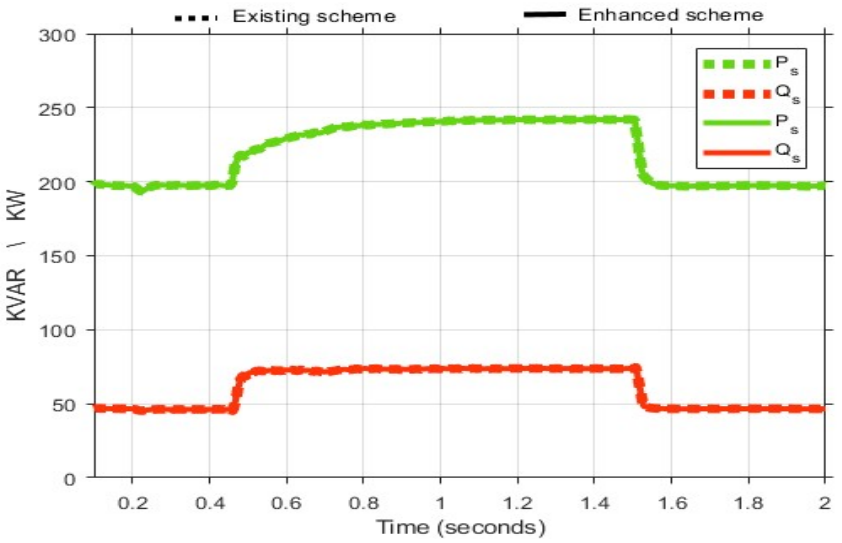

FIGURE 4.7: Real and Reactive power drawn from synchronverter

synchronization process the PCC breaker is closed to allow the power sharing with the grid. It is obvious in Figure 4.6 and 4.7 that when the PCC breaker is closed the rise of current and power was smooth and there is no inrush observed.

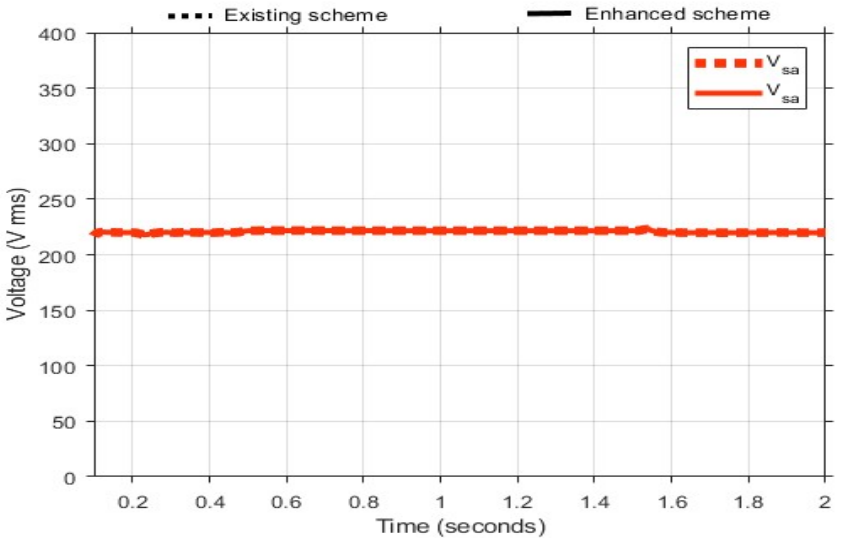

FIGURE 4.8: Synchronverter rms voltages

At 1.5sec, the PCC breaker was opened to test the switching of synchronverter from Grid connected mode to Off Grid mode. There is minimum inrush observed in phase currents during this transfer which shows that the transition was seamless.

It is verified here that the response of both existing and enhanced synchronization schemes remains same when synchronizing with an ideally balanced grid.

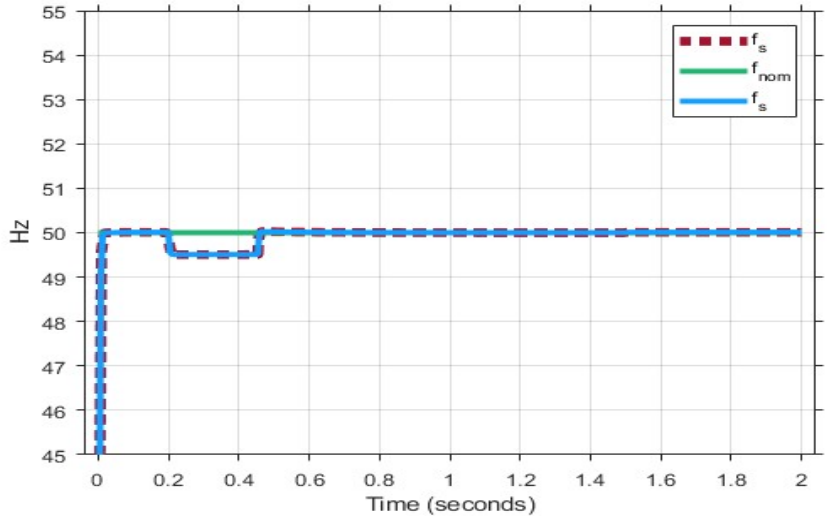

FIGURE 4.9: Synchronverter and nominal frequency

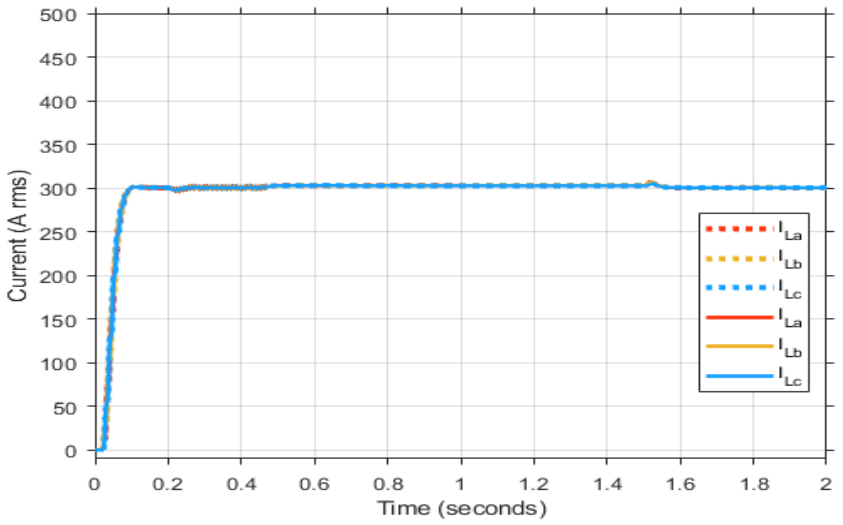

FIGURE 4.10: Local Load current

4.2.2 Pre-synchronization while the Grid Voltage are Unbalanced

This scenario takes an unbalanced power grid that is simulated by a three phase programmable generator by adding negative sequences in the fundamental component ($50Hz$). The negative sequence phase voltage amplitude is $0.05puV$ with phase angle equal to $-30\,\text{deg}$ and it becomes approximately 5% of the positive sequence. The parameters of unbalanced power grid for this scenario are given in Table 4.2.

TABLE 4.2: Parameters of unbalance grid for this scenario.

Grid Phase	Magnitude (RMS)	Phase Angle
Phase a	220 V	0
Phase b	231 V	-120
Phase c	209 V	-240

The magnitude of positive-sequence for this scenario was $220V$ while the magnitude of negative was 0.05pu i.e. $11V$ which corresponds to an unbalance percentage of 5%. The results of this scenario are presented in Figures 4.11 to 4.17. The simulation starts at 0sec.

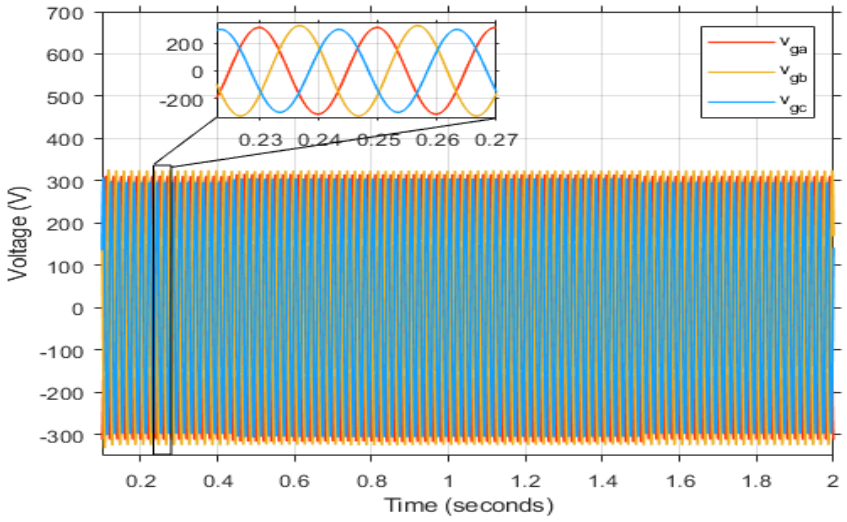

FIGURE 4.11: Grid voltages

After the transient period is over the synchronverter operates in standalone mode maintaining its frequency and voltage at nominal values for the Local load. The unbalance in grid voltage is introduced at 0.1 sec as shown in Figure 4.11. At 0.2 sec the pre-synchronization mode is triggered. The pre-synchronization process is demonstrated in Figure 4.12 which shows that as the frequency of synchronverter is reduced, the voltage difference between all phases of v_s and v_g starts decreasing.

The existing scheme achieves the pre-synchronization $((v_{sa} - v_{ga}) < 12V)$ at 0.423sec whereas the proposed scheme takes 31ms more. The delay in proposed scheme is due to the fact that the magnitude of v_{ga} of unbalanced power grid was lower than its positive sequence v_{ga}^{+}.

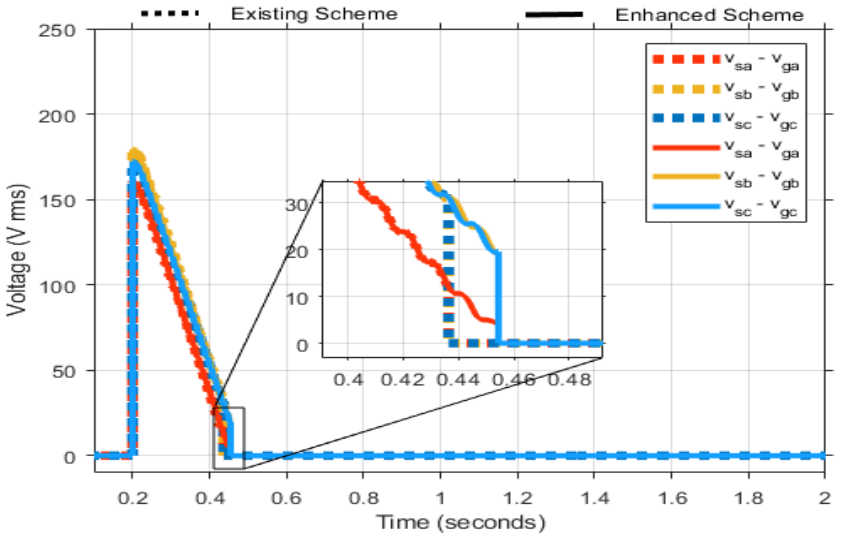

FIGURE 4.12: RMS value of instantaneous difference between synchronverter voltage and grid voltages

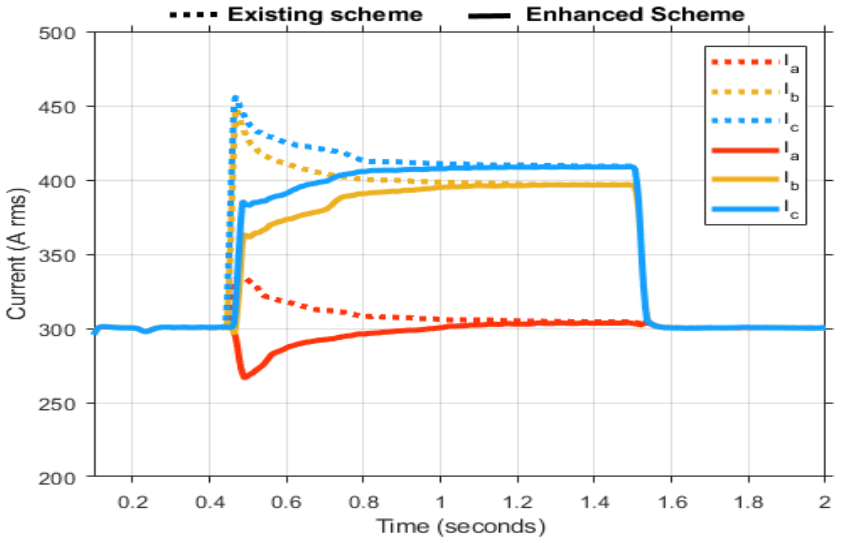

FIGURE 4.13: Synchronverter currents

It can be observed that when pre-synchronization is achieved, the difference $v_{sb} - v_{gb}$ and $v_{sc} - v_{gc}$ is $32V$ and $30V$ in case of existing scheme whereas the proposed scheme reduces it upto $19.2V$ and $18.9V$ respectively which is within limits of international standards of 10% or 22V for grid connection [75].

The curves of inverter current in Figure 4.13 shows that the existing scheme caused high transient currents of 450A and 460A at phase b and c which is almost 50A higher than their steady state values i.e. 400A and 412A respectively. Whereas the proposed scheme has significantly reduced the peak of transient currents. From

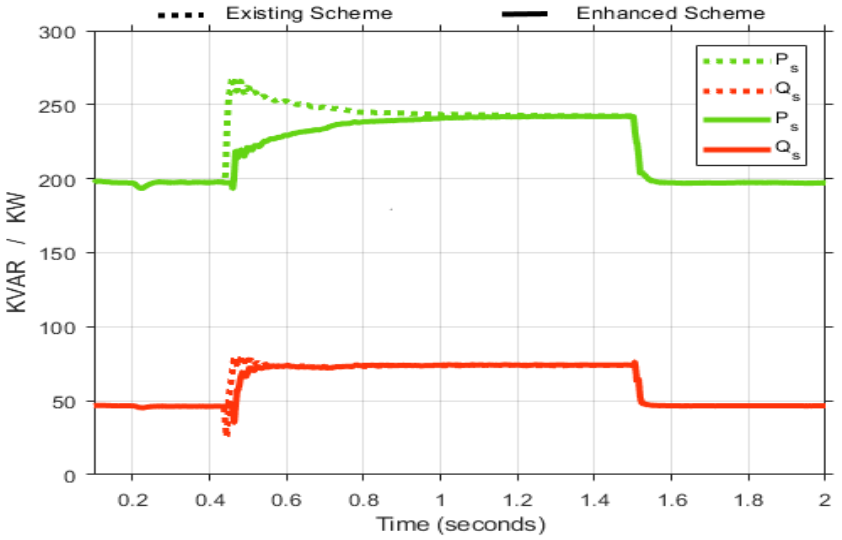

FIGURE 4.14: Real and Reactive power drawn from synchronverter

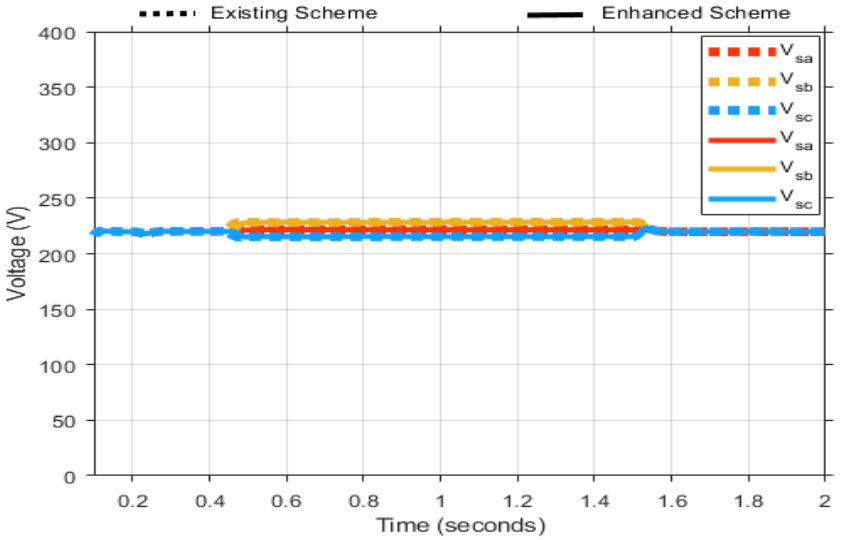

FIGURE 4.15: Synchronverter voltages

Figure 4.14 it is observed that the high transient currents produced by existing scheme caused a significant inrush in the real power P whereas the results of enhanced pre-synchronizer did not show such inrush in P.

The load rms currents in Figure 4.15 shows that during the pre-synchronization process synchronverter continues supply to the Local load. At 1.5sec, the PCC breaker was opened to test the switching of the synchronverter from grid-connected mode to Off-grid mode. The results show that both the schemes can do seamless transfer. In the context of results of this scenario the proposed scheme proved to be

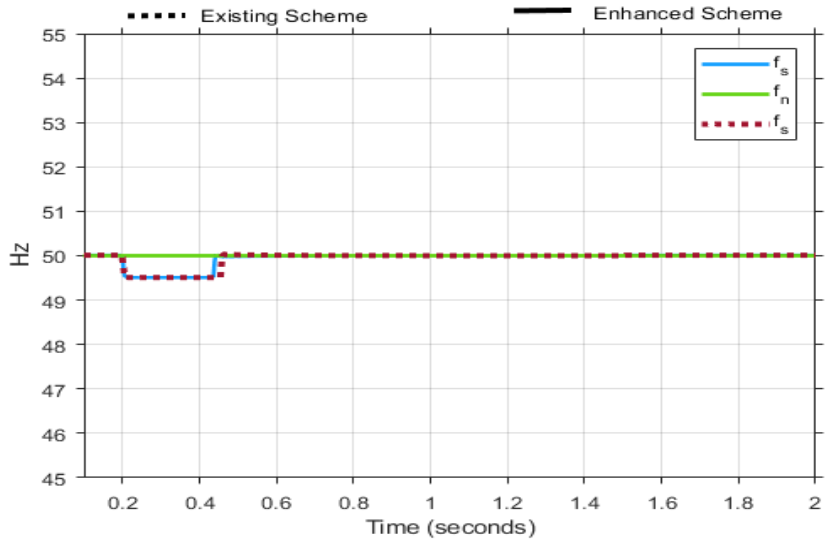

FIGURE 4.16: Synchronverter and nominal frequency

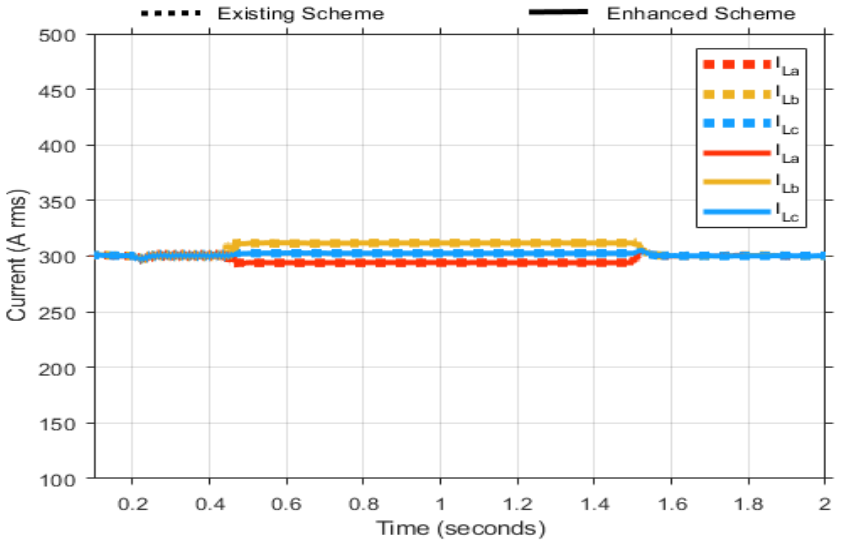

FIGURE 4.17: Local Load current

a better solution for pre-synchronization of synchronverter in practical distribution networks.

4.2.3 Pre-synchronization while the Grid Phase Angles are Unbalanced

In this scenario the performance of existing and enhanced pre-synchronizer is tested with a three phase grid which have equal voltage magnitude but unequal

phase difference. The unbalance in phases is generated by using three single phase AC sources connected in wye configuration. The parameters of unbalanced power grid for this scenario are given in Table 4.3.

TABLE 4.3: Parameters of unbalance grid for this scenario.

Grid Phase	Magnitude (RMS)	Phase Angle
Phase a	220 V	10
Phase b	220 V	-120
Phase c	220 V	-240

The results of this scenario are presented in Figures 4.18 to 4.24. The simulation starts at 0sec. After the transient period is over the synchronverter operates in standalone mode maintaining its frequency and voltage at nominal values for the Local load. The unbalance in grid phase is introduced at 0.1 sec as shown in Figure 4.18. At 0.2 sec the pre-synchronization mode is triggered.

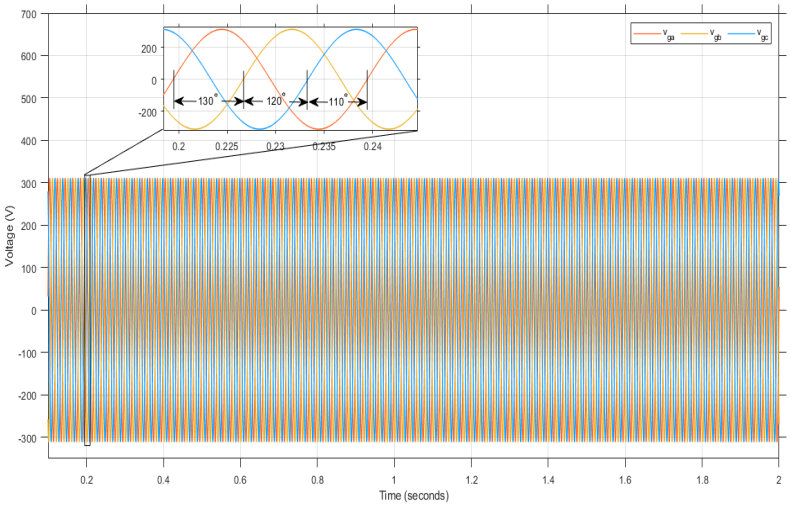

FIGURE 4.18: Grid voltages

The pre-synchronization process is demonstrated in Figure 4.19 which shows that as the frequency of synchronverter is reduced, the voltage difference between all phases of v_s and v_g starts decreasing.

The enhanced scheme achieves the pre-synchronization ($(v_{sa} - v_{ga}) < 12V$) at 0.456sec whereas the existing scheme takes 35ms more. The delay in proposed scheme is due to the fact that the magnitude of v_{ga} of unbalanced power grid was higher than its positive sequence v_{ga}^{+}.

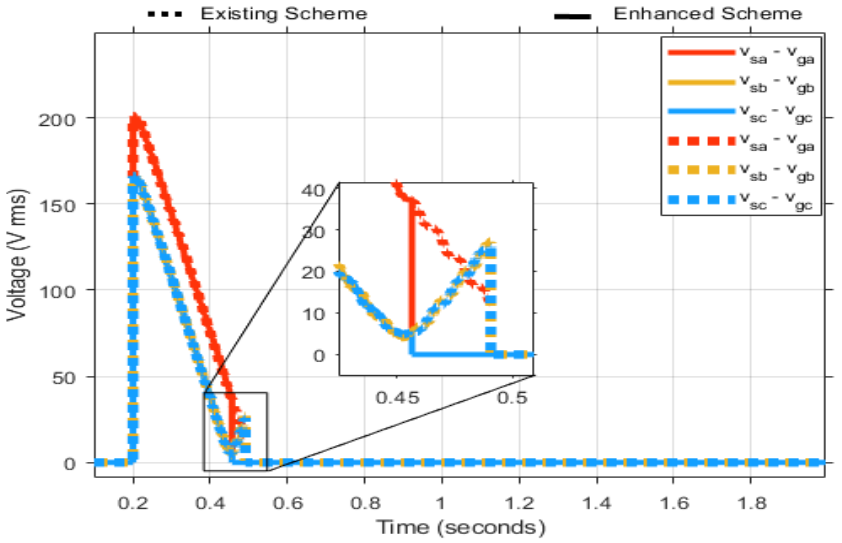

FIGURE 4.19: RMS value of instantaneous difference between synchronverter voltage and grid voltages

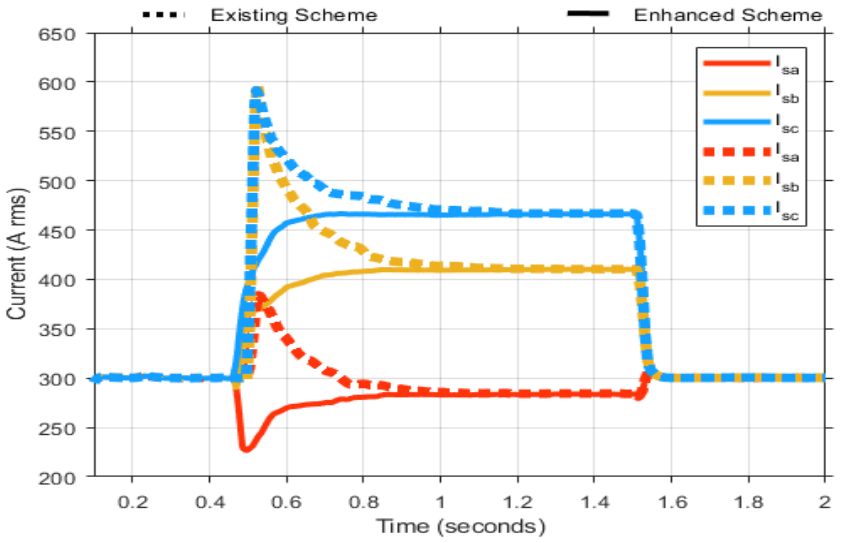

FIGURE 4.20: Synchronverter currents

The curves of inverter current in Figure 4.20 shows that on closing the PCC breaker, the existing scheme caused high transient currents of 595A and 591A at phase b and c which is almost 184A and 123A higher than their steady state values i.e. 411A and 468A respectively. This high transient current can cause over current shutdown of Synchronverter.

Whereas the proposed scheme has no transient peak in synchronverter current. From Figure 4.21 it is observed that the high transient currents produced by existing scheme caused a significant inrush in the real power P whereas the results

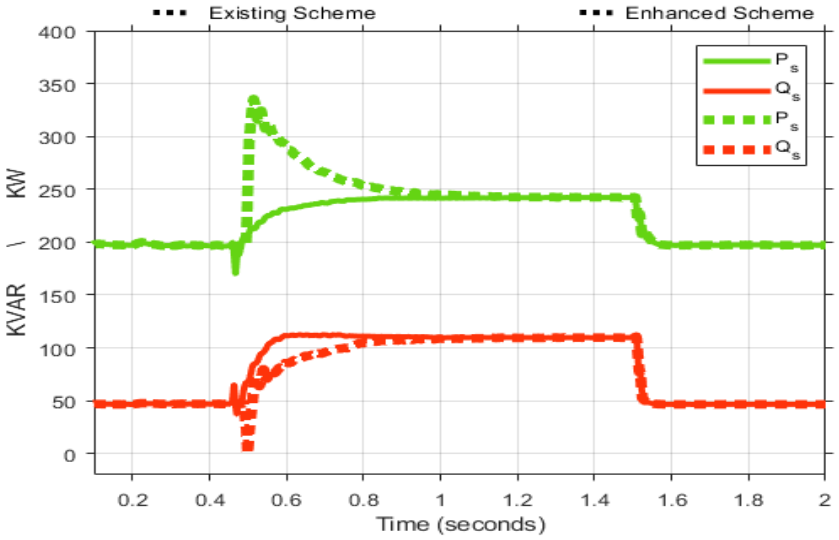

FIGURE 4.21: Real and Reactive power drawn from synchronverter

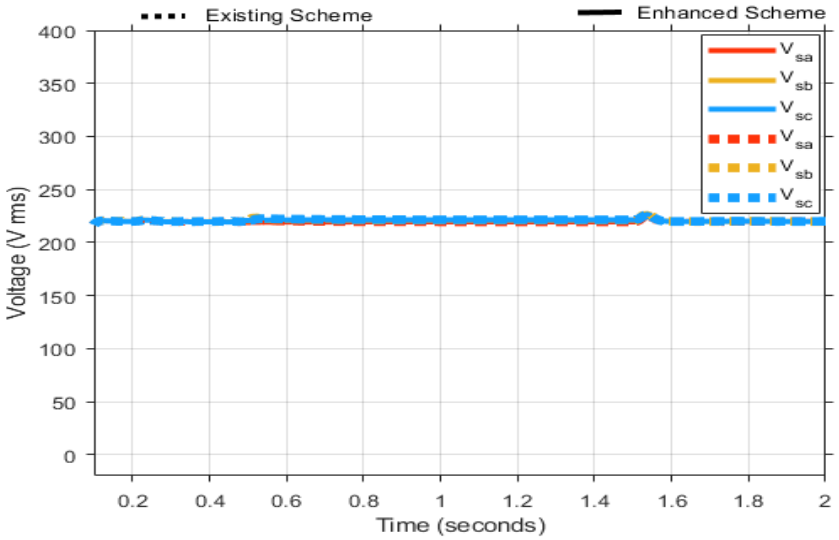

FIGURE 4.22: Synchronverter voltages

of enhanced pre-synchronizer did not show such inrush in P. The load rms currents in Figure 4.22 shows that during the pre-synchronization process synchronverter continues supply to the Local load.

At 1.5sec, the PCC breaker was opened to test the switching of the synchronverter from grid-connected mode to Off-grid mode. The results show that both the schemes can do seamless transfer. In the context of results of this scenario the proposed scheme proved to be a better solution for pre-synchronization of synchronverter in practical distribution networks where there is an unbalance in

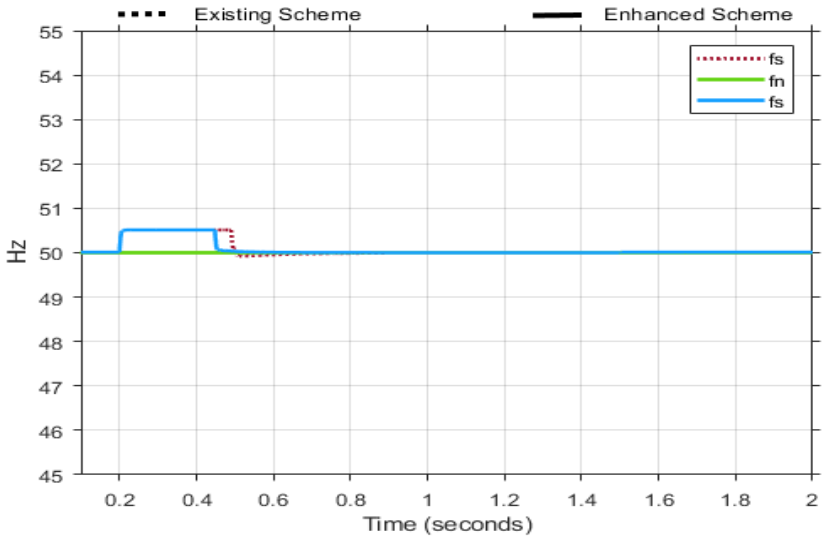

FIGURE 4.23: Synchronverter and nominal frequency

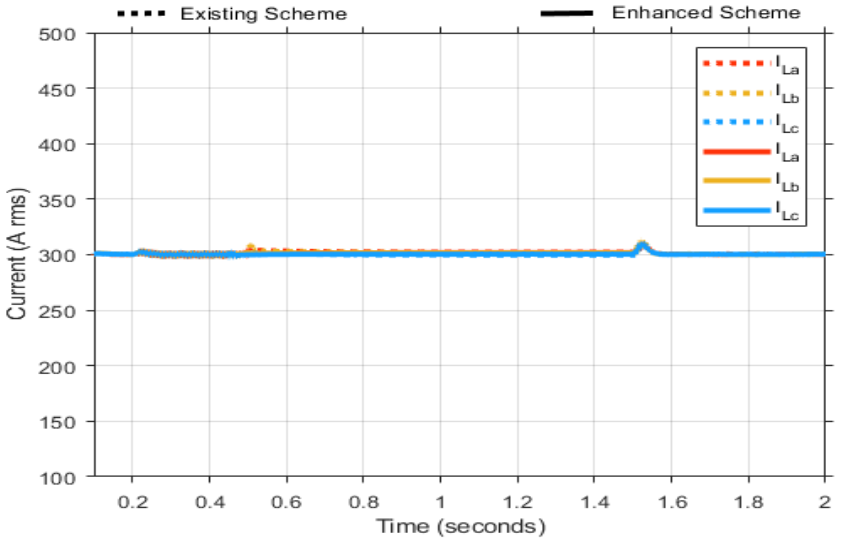

FIGURE 4.24: Local Load currents

phase angle of grid voltages.

4.2.4 Pre-synchronization in Presence of an Unbalanced Sag

The sag is a most frequent power quality issue in power grid. It can be balanced or unbalanced. In this scenario, we are simulating both existing and proposed

schemes to synchronize a synchronverter with the grid in the presence of an unbalanced sag. The sag is generated during the pre-synchronization process by a programmable three-phase source on v_{ga} having duration of 5 cycles. Figure 4.25 to 4.31 shows the results of this scenario.

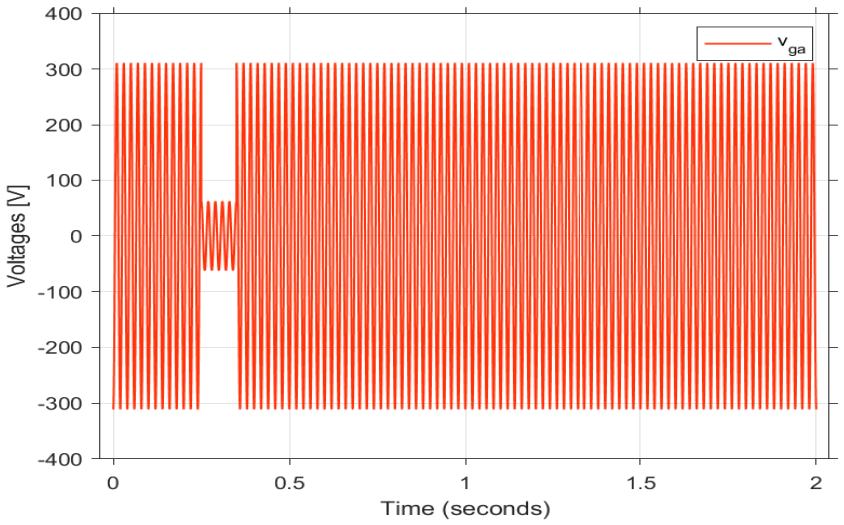

FIGURE 4.25: Grid voltages of Phase a

At 0sec the simulation starts and after the transient period has passed the synchronverter start operating in standalone mode in which it maintains its voltage and frequency at nominal values to maintain the supply for the local load.

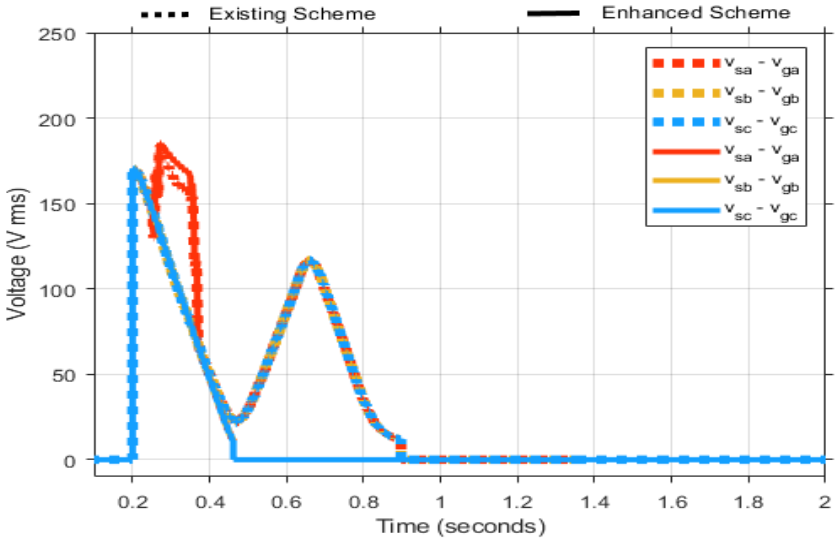

FIGURE 4.26: RMS value of instantaneous difference between synchronverter voltage and grid voltages

The pre-synchronization mode starts at 0.2 sec. As shown in Figure 4.25 the sag occurs at phase a of power grid from 0.25sec to 0.35sec i.e. 5 cycles of 50 Hz nominal frequency. The pre-synchronization process in Figure 4.26 demonstrates that the proposed scheme achieved pre-synchronization within 262 milliseconds, while the existing scheme failed to reduce the voltage difference to the threshold value of $12V$.

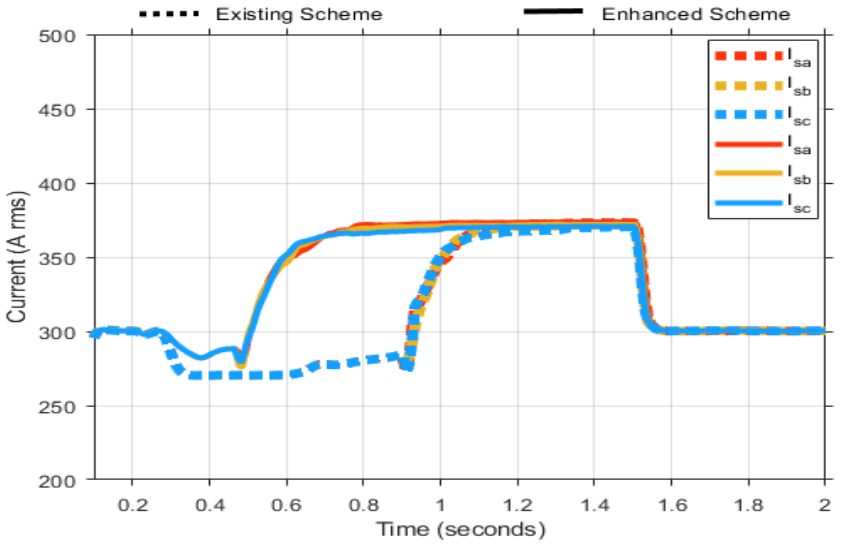

FIGURE 4.27: Synchronverter currents

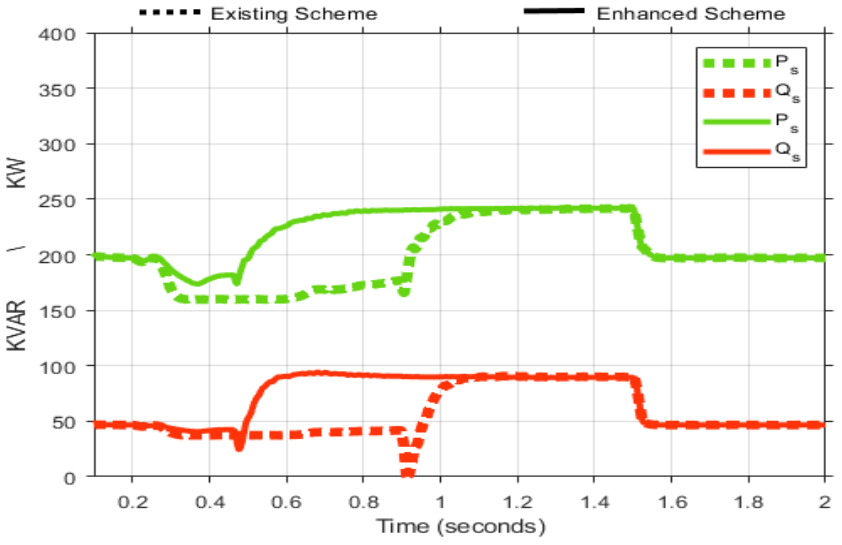

FIGURE 4.28: Real and Reactive power drawn from synchronverter

Instead, it had to repeat the pre-synchronization process when the sag was over, taking a total of 700 milliseconds to achieve pre-synchronization. As the grid is

balanced when the PCC breaker is closed , hence no transient is observed in the inverter currents which can be seen in Figure 4.27.

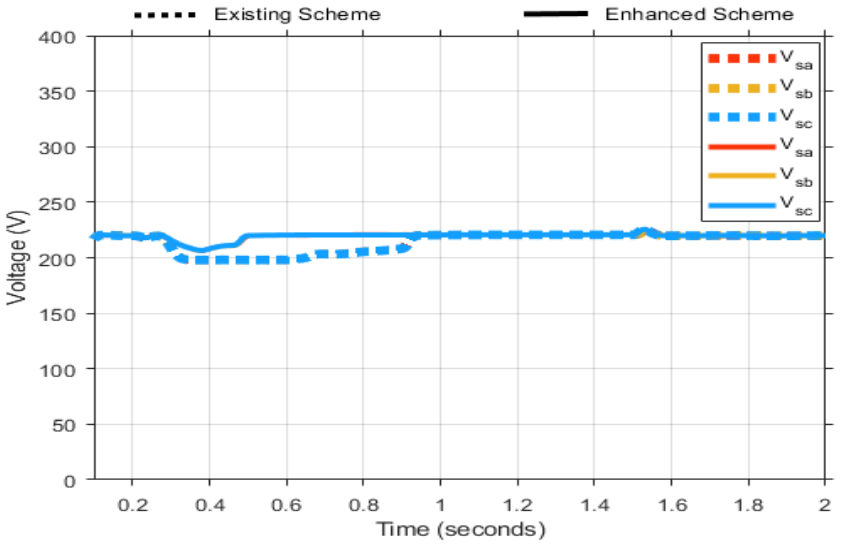

FIGURE 4.29: Synchronverter Voltages

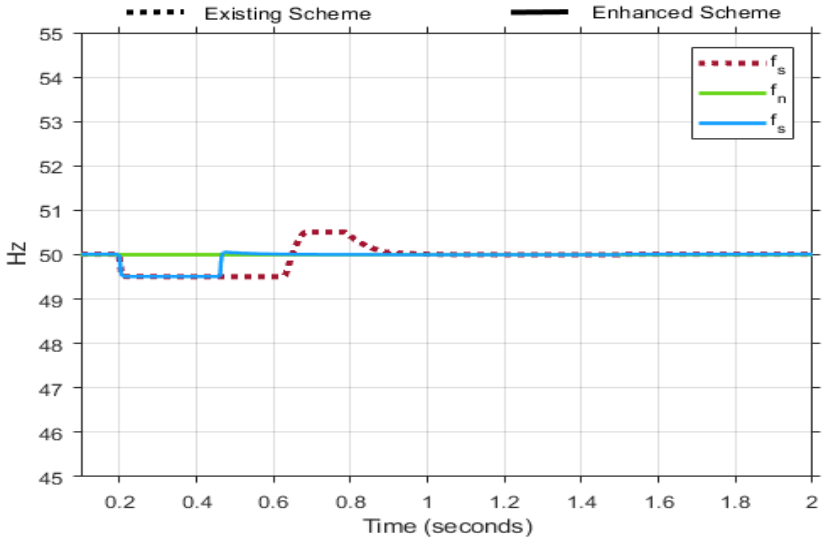

FIGURE 4.30: Synchronverter and nominal frequency

In figure 4.28 it can be observed that both schemes start transferring power to the grid when the PCC breaker closes, but as compared to existing scheme the enhanced pre-synchronizer has causes lower transients in power. The load current curves in Figure 4.29 reveal that the enhanced pre-synchronizer slightly reduces the terminal voltages of synchronverter during pre-synchronization process, whereas the existing scheme causes a significant reduction below 200V in the terminal voltages which also causes reduction in load currents. The results shows that the

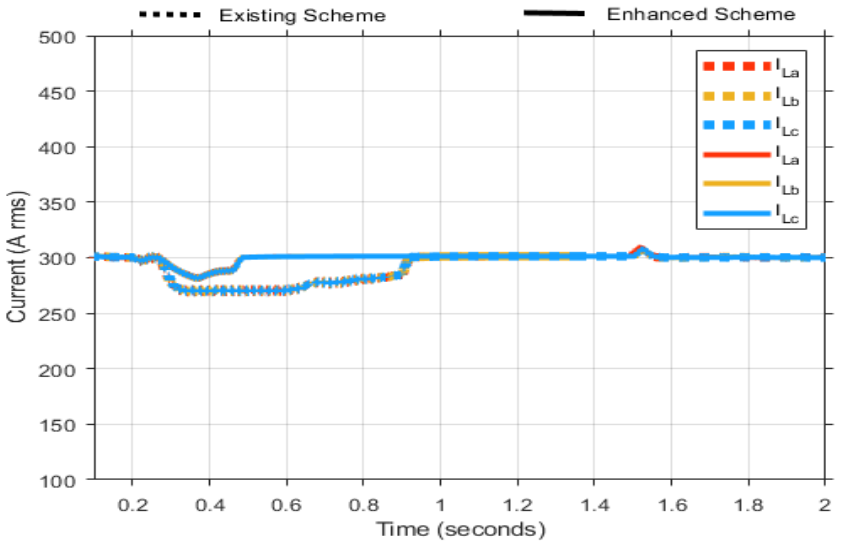

FIGURE 4.31: Local Load currents

enhanced pre-synchronizer can successfully achieve the pre-synchronization if a sag occurs during pre-synchronization whereas the existing scheme has to repeat the pre-synchronization process.

Chapter 5

Conclusion

In this research work, an existing Fourier Analysis based PLL-Less self-synchronizer has been enhanced to achieve seamless pre-synchronization of synchronverter with an unbalanced grid. The enhanced pre-synchronizer is designed and tested in Simulink/MATLAB 2023 in different scenarios of power grid. The enhanced pre-synchronizer gives an improved performance as described in following points.

1. The enhanced pre-synchronizer can achieve a hot-seamless synchronization with a balanced as well as unbalanced power grid

2. As compared to existing scheme, the enhanced pre-synchronizer can reduce the voltage difference at PCC, during pre-synchronization if the power grid has an unbalance in its voltage. This reduced voltage difference gives the advantage of reduced inrush in synchronverter current and power.

3. If the power grid has a phase angle imbalance among its phases, the enhanced pre-synchronizer completely removes the high inrush in synchronverter currents when the PCC breaker is closed. While the existing scheme produces very high inrush currents which can cause over current tripping of synchronverter.

4. The enhanced pre-synchronizer has a capability of achieving faster pre-synchronization while an unbalanced sag occurs in power grid.

Thus after the modification, the existing FA-based PLL-Less pre-synchronizer has become capable to achieve a hot-seamless pre-synchronization of synchronverter with unbalanced power grid.

5.1 Future Directions

In future , this research can be extended in many directions as discussed below.

- The performance of the synchronverter can be assessed by connecting solar panels or other renewable resources to the DC side of the synchronverter, instead of using an ideal DC source as was done in this research.
- The results obtained during this research work are simulations based. For concrete results, the performance of synchronverter with enhanced pre-synchronizer can be tested on an experimental setup.
- In some applications, it is required to run small rated inverters in parallel. Therefore, the performance of enhanced pre-synchronizer can be evaluated for parallel operation of synchronverters in a weak grid.
- The synchronverter is being used in microgrids as a grid forming converter for grid pre-synchronization where it has to operate with other type of inverters. Therefore, the synchronverter with enhanced pre-synchronizer can be evaluated in Microgrids for pre-synchronization with an unbalanced grid.

Bibliography

[1] R. Lowe and P. Drummond, "Solar, wind and logistic substitution in global energy supply to 2050–barriers and implications," *Renewable and Sustainable Energy Reviews*, vol. 153, p. 111720, 2022.

[2] S. Algarni, V. Tirth, T. Alqahtani, S. Alshehery, and P. Kshirsagar, "Contribution of renewable energy sources to the environmental impacts and economic benefits for sustainable development," *Sustainable Energy Technologies and Assessments*, vol. 56, p. 103098, 2023.

[3] N. Mammadov, N. Ganiyeva, and G. Aliyeva, "Role of renewable energy sources in the world," *Journal of Renewable Energy, Electrical, and Computer Engineering*, vol. 2, no. 2, pp. 63–67, 2022.

[4] A. O. Maka and J. M. Alabid, "Solar energy technology and its roles in sustainable development," *Clean Energy*, vol. 6, no. 3, pp. 476–483, 2022.

[5] X. Ding, L. Liu, G. Huang, Y. Xu, and J. Guo, "A multi-objective optimization model for a non-traditional energy system in beijing under climate change conditions," *Energies*, vol. 12, no. 9, p. 1692, 2019.

[6] S. Minazhova, R. Akhambayev, T. Shalabayev, A. Bekbayev, B. Kozhageldi, and M. Tvaronavičienė, "A review on solar energy policy and current status: Top 5 countries and kazakhstan," *Energies*, vol. 16, no. 11, 2023. [Online]. Available: https://www.mdpi.com/1996-1073/16/11/4370

[7] H. Sun, R. U. Awan, M. A. Nawaz, M. Mohsin, A. K. Rasheed, and N. Iqbal, "Assessing the socio-economic viability of solar commercialization and electrification in south asian countries," *Environment, Development and Sustainability*, vol. 23, pp. 9875–9897, 2021.

[8] "Energy resources, National Transmission and Dispatch Company (NTDC)," 2018, Accessed on 29-11-2021. [Online]. Available: https://ntdc.gov.pk/energy

[9] "Current status of solar PV power projects," 2021, Accessed on 29-11-2021. [Online]. Available: https://www.aedb.org/ae-technologies/solar-power/solar-current-status

[10] "Annual report 2020-21, National Electric Power Regulatory Authority (NEPRA)," 2021, Accessed on 29-11-2021. [Online]. Available: https://nepra.org.pk/publications/Annual%20Reports/Annual%20Report%202020-21.pdf

[11] U. Tamrakar, D. Shrestha, M. Maharjan, B. P. Bhattarai, T. M. Hansen, and R. Tonkoski, "Virtual inertia: Current trends and future directions," *Applied sciences*, vol. 7, no. 7, p. 654, 2017.

[12] X. Li, Z. Wang, L. Zhang, F. Sun, D. Cui, C. Hecht, J. Figgener, and D. U. Sauer, "Electric vehicle behavior modeling and applications in vehicle-grid integration: An overview," *Energy*, vol. 268, p. 126647, 2023. [Online]. Available: https://www.sciencedirect.com/science/article/pii/S0360544223000415

[13] B. Muftau and M. Fazeli, "The role of virtual synchronous machines in future power systems: A review and future trends," *Electric Power Systems Research*, vol. 206, p. 107775, 2022.

[14] S. A. Khan, M. Wang, W. Su, G. Liu, and S. Chaturvedi, "Grid-forming converters for stability issues in future power grids," *Energies*, vol. 15, no. 14, p. 4937, 2022.

[15] R. Shi and X. Zhang, "Vsg-based dynamic frequency support control for autonomous pv–diesel microgrids," *Energies*, vol. 11, no. 7, p. 1814, 2018.

[16] S. Rahman, S. Saha, S. N. Islam, M. T. Arif, M. Mosadeghy, M. Haque, and A. M. Oo, "Analysis of power grid voltage stability with high penetration of solar pv systems," *IEEE Transactions on Industry Applications*, vol. 57, no. 3, pp. 2245–2257, 2021.

[17] M. Bajaj and A. K. Singh, "Grid integrated renewable dg systems: A review of power quality challenges and state-of-the-art mitigation techniques," *International Journal of Energy Research*, vol. 44, no. 1, pp. 26–69, 2020.

[18] H. Husin, M. Zaki *et al.*, "A critical review of the integration of renewable energy sources with various technologies," *Protection and control of modern power systems*, vol. 6, no. 1, pp. 1–18, 2021.

[19] Q.-C. Zhong and G. Weiss, "Synchronverters: Inverters that mimic synchronous generators," *IEEE transactions on industrial electronics*, vol. 58, no. 4, pp. 1259–1267, 2010.

[20] J. Liu, D. Yang, W. Yao, R. Fang, H. Zhao, and B. Wang, "Pv-based virtual synchronous generator with variable inertia to enhance power system transient stability utilizing the energy storage system," *Protection and Control of Modern Power Systems*, vol. 2, pp. 1–8, 2017.

[21] M. Shadoul, R. Ahshan, R. S. AlAbri, A. Al-Badi, M. Albadi, and M. Jamil, "A comprehensive review on a virtual-synchronous generator: Topologies, control orders and techniques, energy storages, and applications," *Energies*, vol. 15, no. 22, 2022. [Online]. Available: https://www.mdpi.com/1996-1073/15/22/8406

[22] J. D. A. de Oliveira, F. K. de Araújo Lima, F. L. Tofoli, and C. G. C. Branco, "Synchronverter-based frequency control technique applied in wind energy conversion systems based on the doubly-fed induction generator," *Electric Power Systems Research*, vol. 214, p. 108820, 2023.

[23] F. Wald, Q. Tao, and G. De Carne, "Virtual synchronous machine control for asynchronous grid connections," *IEEE Transactions on Power Delivery*, vol. 39, no. 1, pp. 397–406, 2023.

[24] M. Shadoul, R. Ahshan, R. S. AlAbri, A. Al-Badi, M. Albadi, and M. Jamil, "A comprehensive review on a virtual-synchronous generator: Topologies, control orders and techniques, energy storages, and applications," *Energies*, vol. 15, no. 22, p. 8406, 2022.

[25] C. Zhong, H. Li, Y. Zhou, Y. Lv, J. Chen, and Y. Li, "Virtual synchronous generator of pv generation without energy storage for frequency support in autonomous microgrid," *International Journal of Electrical Power & Energy Systems*, vol. 134, p. 107343, 2022.

[26] C. Verdugo, A. Tarraso, J. I. Candela, J. Rocabert, and P. Rodriguez, "Centralized synchronous controller based on load angle regulation for photovoltaic power plants," *IEEE journal of emerging and selected topics in power electronics*, vol. 9, no. 1, pp. 485–496, 2020.

[27] S. Agrawal, B. Tyagi, V. Kumar, and P. Sharma, "Enhancing grid stability through adaptive damping and inertia control in dfig-based wind turbines with vsync," in *2023 IEEE International Conference on Energy Technologies for Future Grids (ETFG)*. IEEE, 2023, pp. 1–5.

[28] Q.-C. Zhong, P.-L. Nguyen, Z. Ma, and W. Sheng, "Self-synchronized synchronverters: Inverters without a dedicated synchronization unit," *IEEE Transactions on power electronics*, vol. 29, no. 2, pp. 617–630, 2013.

[29] P. Lorenzetti, Z. Kustanovich, S. Shivratri, and G. Weiss, "The equilibrium points and stability of grid-connected synchronverters," *IEEE Transactions on Power Systems*, vol. 37, no. 2, pp. 1184–1197, 2021.

[30] K. R. Vasudevan, V. K. Ramachandaramurthy, T. S. Babu, and A. Pouryekta, "Synchronverter: A comprehensive review of modifications, stability assessment, applications and future perspectives," *IEEE Access*, vol. 8, pp. 131 565–131 589, 2020.

[31] P. Kundur, *Power System Stability and Control*, 1st ed. McGraw-Hill, 1994.

[32] S. Chapman, *Electric Machinery Fundamentals*, 5th ed. McGraw-Hill, 2012.

[33] W. Zhang, D. Remon, and P. Rodriguez, "Frequency support characteristics of gridinteractive power converters based on the synchronous power controller," *IET Renewable Power Generation*, vol. 11, no. 4, pp. 470–479, 2017.

[34] Q. C. Zhong, P.-L. P. Nguyen, Z. Ma, and W. Sheng, "Self-synchronised synchronverters: Inverters without a dedicated synchronisation unit," *IEEE Transactions on Power Electronics*, vol. 29, no. 2, pp. 617–630, 2014.

[35] M. Ashabani and Y. A. R. I. Mohamed, "Novel comprehensive control framework for incorporating VSCs to smart power grids using bidirectional synchronous-VSC," *IEEE Transactions on Power Systems*, vol. 29, no. 2, pp. 943–957, 2014.

[36] V. Natarajan and G. Weiss, "Synchronverters with better stability due to virtual inductors, virtual capacitors, and anti-windup," *IEEE Transactions on Industrial Electronics*, vol. 64, no. 7, pp. 5994–6004, 2017.

[37] Z. Shuai, W. Huang, C. Shen, J. Ge, and Z. J. Shen, "Characteristics and restraining method of fast transient inrush fault currents in synchronverters," *IEEE Transactions on Industrial Electronics*, vol. 64, no. 9, pp. 7487–7497, 2017.

[38] T. Shao, T. Q. Zheng, H. Li, and X. Zhang, "Parameter design and hot seamless transfer of single-phase synchronverter," *Electric Power Systems Research*, vol. 160, pp. 63–70, 2018.

[39] Q. C. Zhong, G. C. Konstantopoulos, B. Ren, and M. Krstic, "Improved synchronverters with bounded frequency and voltage for smart grid integration," *IEEE Transactions on Smart Grid*, vol. 9, no. 2, pp. 786–796, 2018.

[40] X. Wang, L. Chen, D. Sun, L. Zhang, and H. Nian, "A modified self-synchronized synchronverter in unbalanced power grids with balanced currents and restrained power ripples," *Energies*, vol. 12, no. 5, p. 923, 2019.

[41] G. C. Kryonidis, K.-N. D. Malamaki, J. M. Mauricio, and C. S. Demoulias, "A new perspective on the synchronverter model," *International Journal of Electrical Power & Energy Systems*, vol. 140, pp. 1–12, 2022.

[42] H. Yin, Z. Kustanovich, and G. Weiss, "Attenuation of power system oscillations by using virtual damper windings," in *2022 IEEE 23rd Workshop on Control and Modeling for Power Electronics (COMPEL)*. IEEE, 2022, pp. 1–6.

[43] C. Busada, S. G. Jorge, and J. A. Solsona, "Current-controlled synchronverter: A grid fault tolerant grid forming inverter," *IEEE Transactions on Industrial Electronics*, vol. 71, no. 4, pp. 3233–3241, 2023.

[44] Z. Kustanovich, S. Shivratri, H. Yin, F. Reissner, and G. Weiss, "Synchronverters with fast current loops," *IEEE Transactions on Industrial Electronics*, vol. 70, no. 11, pp. 11 357–11 367, 2023.

[45] S. Dong and Y. C. Chen, "Adjusting synchronverter dynamic response speed via damping correction loop," *IEEE Transactions on Energy Conversion*, vol. 32, no. 2, pp. 608–619, 2017.

[46] M. Naeem and U. A. Khan, "A pll-less fourier analysis based self-synchronizer for synchronverter having uninterrupted power supply capability," *e-Prime - Advances in Electrical Engineering, Electronics and Energy*, vol. 5, p. 100257, 2023. [Online]. Available: https://www.sciencedirect.com/science/article/pii/S2772671123001523

[47] "An enhanced auto-synchronizer for integration of the virtual synchronous machine into power grid," 2022, Accessed on 08-07-2024. [Online]. Available: https://cust.edu.pk/wp-content/uploads/2023/33%20PhD%20Theses/PhD%20EE%20Thesis%20Muhammad%20Naeem.pdf

[48] S. M. Ashabani and Y. A. R. I. Mohamed, "A flexible control strategy for grid-connected and islanded microgrids with enhanced stability using nonlinear microgrid stabilizer," *IEEE Transactions on Smart Grid*, vol. 3, no. 3, pp. 1291–1301, 2012.

[49] Q. C. Zhong, Z. Ma, W. L. Ming, and G. C. Konstantopoulos, "Grid-friendly wind power systems based on the synchronverter technology," *Energy Conversion and Management*, vol. 89, pp. 719–726, 2015.

[50] Q. Tan, Z. Lv, B. Xu, W. Jiang, X. Ai, and Q. C. Zhong, "A novel three-phase four-wire grid-connected synchronverter that mimics synchronous generators," *Journal of Power Electronics*, vol. 16, no. 6, pp. 2221–2230, 2016.

[51] D. Dong, B. Wen, D. Boroyevich, P. Mattavelli, and Y. Xue, "Analysis of phase locked loop low frequency stability in three phase grid connected power converters considering impedance interactions," *IEEE Transactions on Industrial Electronics*, vol. 62, no. 1, pp. 310–321, 2015.

[52] L. Huang, H. Xin, Z. Wang, K. Wu, H. Wang, J. Hu, and C. Lu, "A virtual synchronous control for voltage source converters utilizing dynamics of DC-link capacitor to realize self-synchronization," *IEEE Transactions on emerging and selected topics in power electronics*, vol. 5, no. 4, pp. 1565–1577, 2017.

[53] M. R. Amin and S. A. Zulkifli, "A framework for selection of grid-inverter synchronisation unit: Harmonics, phase-angle and frequency," *Renewable and Sustainable Energy Reviews*, vol. 78, pp. 210–219, 2017.

[54] K. Y. Yap, C. R. Sarimuthu, and J. M.-Y. Lim, "Virtual inertia-based inverters for mitigating frequency instability in grid-connected renewable energy system: A review," *Applied Sciences*, vol. 9, no. 24, pp. 1–29, 2019.

[55] M. Amin, A. Rygg, and M. Molinas, "Self-synchronization of wind farm in MMC-based HVDC system: A stability investigation," *IEEE Transactions on Energy Conversion*, vol. 32, no. 2, pp. 458–470, 2017.

[56] T. Younis, M. Ismeil, E. K. Hussain, and M. Orabi, "An improved single-phase self-synchronized synchronverter with enhanced dynamics and current limitation capability," *IET Power Electronics*, vol. 12, no. 2, pp. 337–344, 2019.

[57] R. Pérez, A. R. Cabero, and M. Prodanovic, "Harmonic virtual impedance design for parallel-controlled grid-tied synchronverters," *IEEE Journal of Emerging and Selected Topics in Power Electronics*, vol. 7, no. 1, pp. 493–503, 2019.

[58] Q. C. Zhong, W.-L. Ming, and Y. Zeng, "Self-synchronized universal droop controller," *IEEE Access*, vol. 4, pp. 7145–7153, 2016.

[59] S. Dong, J. Jiang, and Y. C. Chen, "Analysis of synchronverter self-synchronization dynamics to facilitate parameter tuning," *IEEE Transactions on Energy Conversion*, vol. 35, no. 1, pp. 11–23, 2020.

[60] S. Dong and Y. C. Chen, "A fast self-synchronizing synchronverter design with easily tuneable parameters," in *IEEE Power and Energy Society General Meeting (PESGM)*, Portland, August 2018, pp. 1–5.

[61] M. J. Quintero-Duran, J. E. Candelo-Becerra, and J. Posada, "Synchronizing a synchronverter to an unbalanced power grid using sequence component decomposition," *Nonlinear Engineering*, vol. 11, no. 1, pp. 395–410, 2022.

[62] C. L. Fortescue, "Method of symmetrical co-ordinates applied to the solution of polyphase networks," *Transactions of the American Institute of Electrical Engineers*, vol. 37, no. 2, pp. 1027–1140, 1918.

[63] W. V. Lyon, "Applications of the method of symmetrical components," *(No Title)*, 1937.

[64] R. Hariharan and M. K. Mishra, "An integrated control of enhanced-pll and synchronverter for unbalanced grid," *IEEE Transactions on Industry Applications*, vol. 58, no. 2, pp. 2206–2216, 2021.

[65] R. V. Ferreira, S. M. Silva, and D. I. Brandao, "Positive-negative sequence synchronverter for unbalanced voltage in ac grids," *Journal of Control, Automation and Electrical Systems*, vol. 32, pp. 711–720, 2021.

[66] V. R. Chowdhury and D. Divan, "Lyapunov energy function based direct power control of synchronverters under unbalanced grid voltage conditions,"

in *2021 IEEE Energy Conversion Congress and Exposition (ECCE)*. IEEE, 2021, pp. 992–999.

[67] G. Barzilai, L. Marcus, and G. Weiss, "Energy storage systems—grid connection using synchronverters," in *2016 IEEE International Conference on the Science of Electrical Engineering (ICSEE)*. IEEE, 2016, pp. 1–5.

[68] J. Roldán-Pérez, M. Prodanovic, and A. Rodríguez-Cabero, "Detailed discrete-time implementation of a battery-supported synchronverter for weak grids," in *IECON 2017-43rd Annual Conference of the IEEE Industrial Electronics Society*. IEEE, 2017, pp. 1083–1088.

[69] K. Y. Yap, H. Y. Hon, and C. R. Sarimuthu, "Grid integration of solar power system using synchronverter-based energy storage system," *Applied Solar Energy*, vol. 58, no. 3, pp. 444–457, 2022.

[70] A. J. Sonawane and A. C. Umarikar, "Voltage and reactive power regulation with synchronverter-based control of pv-statcom," *IEEE Access*, vol. 11, pp. 52 129–52 140, 2023.

[71] ——, "Three-phase single-stage photovoltaic system with synchronverter control: Power system simulation studies," *IEEE Access*, vol. 10, pp. 23 408–23 424, 2022.

[72] K. Y. Yap, C. R. Sarimuthu, and J. M.-Y. Lim, "Grid integration of solar photovoltaic system using machine learning-based virtual inertia synthetization in synchronverter," *IEEE Access*, vol. 8, pp. 49 961–49 976, 2020.

[73] Q.-C. Zhong, Z. Ma, W.-L. Ming, and G. C. Konstantopoulos, "Grid-friendly wind power systems based on the synchronverter technology," *Energy Conversion and Management*, vol. 89, pp. 719–726, 2015.

[74] D. F. Pereira, L. F. N. Lourenço, R. M. Monaro, M. B. C. Salles, and V. Z. Silva, "Synchronverter-based hvdc transmission for an isolated offshore grid based on the power hub concept," *Available at SSRN 4353964*.

[75] G. Wu, J. Liang, X. Zhou, Y. Li, A. Egea-Alvarez, G. Li, H. Peng, and X. Zhang, "Analysis and design of vector control for vsc-hvdc connected to weak grids," *CSEE Journal of Power and Energy Systems*, vol. 3, no. 2, pp. 115–124, 2017.

[76] Z. Ma, Q.-C. Zhong, and J. D. Yan, "Synchronverter-based control strategies for three-phase pwm rectifiers," in *2012 7th IEEE conference on industrial electronics and applications (ICIEA)*. IEEE, 2012, pp. 225–230.

[77] R. A. [2]Bogdan MARINESCU, K. B. KILANI, and M. ELLEUCH, "Stability improvement of the interconnection of weak ac zones by synchronverter-based hvdc link."

[78] R. Aouini, B. Marinescu, K. B. Kilani, and M. Elleuch, "Synchronverter-based emulation and control of hvdc transmission," *IEEE Transactions on Power Systems*, vol. 31, no. 1, pp. 278–286, 2015.

[79] L. do Nascimento Gomes, A. J. G. Abrantes-Ferreira, R. F. da Silva Dias, and L. G. B. Rolim, "Synchronverter-based statcom with voltage imbalance compensation functionality," *IEEE Transactions on Industrial Electronics*, vol. 69, no. 5, pp. 4836–4844, 2021.

[80] P.-L. Nguyen, Q.-C. Zhong, F. Blaabjerg, and J. M. Guerrero, "Synchronverter-based operation of statcom to mimic synchronous condensers," in *2012 7th IEEE conference on industrial electronics and applications (ICIEA)*. IEEE, 2012, pp. 942–947.

[81] J. A. Sanguesa, V. Torres-Sanz, P. Garrido, F. J. Martinez, and J. M. Marquez-Barja, "A review on electric vehicles: Technologies and challenges," *Smart Cities*, vol. 4, no. 1, pp. 372–404, 2021.

[82] D. Liu, Q. Zhong, Y. Wang, and G. Liu, "Modeling and control of a v2g charging station based on synchronverter technology," *CSEE Journal of Power and Energy Systems*, vol. 4, no. 3, pp. 326–338, 2018.

[83] T. Yang and W. Hu, "Research on variable inertia control strategy of electric vehicle based on synchronverter," in *2021 IEEE 4th International Electrical and Energy Conference (CIEEC)*. IEEE, 2021, pp. 1–6.

[84] V. F. Pires, A. Pires, and A. Cordeiro, "Dc microgrids: benefits, architectures, perspectives and challenges," *Energies*, vol. 16, no. 3, p. 1217, 2023.

[85] S. Peyghami, P. Davari, H. Mokhtari, P. C. Loh, and F. Blaabjerg, "Synchronverter-enabled dc power sharing approach for lvdc microgrids," *IEEE Transactions on Power Electronics*, vol. 32, no. 10, pp. 8089–8099, 2016.

[86] M. A. Azzouz, H. H. Zeineldin, and E. F. El-Saadany, "Selective phase tripping for microgrids powered by synchronverter-interfaced renewable energy sources," *IEEE Transactions on Power Delivery*, vol. 36, no. 6, pp. 3506–3518, 2020.

[87] M. J. Quintero-Duran, J. E. Candelo-Becerra, and J. Posada, "Synchronizing a synchronverter to an unbalanced power grid using sequence component decomposition," *Nonlinear Engineering*, vol. 11, no. 1, pp. 395–410, 2022. [Online]. Available: https://doi.org/10.1515/nleng-2022-0043

[88] I. Bennia, Y. Daili, and A. Harrag, "Lcl filter design for low voltage-source inverter," in *Artificial Intelligence and Heuristics for Smart Energy Efficiency in Smart Cities: Case Study: Tipasa, Algeria*. Springer, 2022, pp. 332–341.

[89] X. Yang, M. Alathamneh, and R. Nelms, "Improved lcl filter design procedure for grid-connected voltage-source inverter system," in *2021 IEEE Energy Conversion Congress and Exposition (ECCE)*. IEEE, 2021, pp. 3587–3591.

[90] C.-K. Nguyen, T.-T. Nguyen, H.-J. Yoo, and H.-M. Kim, "Improving transient response of power converter in a stand-alone microgrid using virtual synchronous generator," *Energies*, vol. 11, no. 1, 2018. [Online]. Available: https://www.mdpi.com/1996-1073/11/1/27

[91] Q. Tan, Z. Lv, B. Xu, W. Jiang, X. Ai, and Q. Zhong, "A novel three-phase four-wire grid-connected synchronverter that mimics synchronous generators," *Journal of power electronics*, vol. 16, no. 6, pp. 2221–2230, 2016.